SCIENCE CHINA
Information Sciences

• RESEARCH PAPER •

January 2023, Vol. 66 112202:1–112202:22
https://doi.org/10.1007/s11432-021-3434-9

Pattern-based learning and control of nonlinear pure-feedback systems with prescribed performance

Fukai ZHANG, Weiming WU & Cong WANG*

Center for Intelligent Medical Engineering, School of Control Science and Engineering, Shandong University, Jinan 250061, *China*

Received 8 June 2021/Revised 24 November 2021/Accepted 24 January 2022/Published online 26 December 2022

Abstract This article presents a novel pattern-based intelligent control scheme with prescribed performance (PP) for uncertain pure-feedback systems operating in multiple control situations (patterns). Based on PP, an observer-based adaptive neural network (NN) control approach, which not only achieves system stability and prescribed tracking control performance but also realizes accurate identification/learning of the unknown closed-loop dynamics via deterministic learning and uses only one NN unit, is proposed. Subsequently, the knowledge learned is utilized to construct high-performance candidate controllers for each control situation. Based on the transformed system and observer technique, accurate classification of the nth order systems under different control situations is achieved by requiring only one set of dynamic estimators, thereby significantly reducing the complexity of pattern recognition. Thus, sudden changes in the control situation can be rapidly recognized based on the minimum residual principle, with which the correct candidate controller is selected to achieve superior control performance. The simulation results verify the efficacy of the proposed scheme.

Keywords adaptive neural control (ANC), deterministic learning, neural networks (NNs), pattern-based control, high gain observer, pure-feedback systems

Citation Zhang F K, Wu W M, Wang C. Pattern-based learning and control of nonlinear pure-feedback systems with prescribed performance. Sci China Inf Sci, 2023, 66(1): 112202, https://doi.org/10.1007/s11432-021-3434-9

1 Introduction

In the real world, humans can learn many highly complex control tasks with sufficient practice, and the same control task or a similar control task encountered the next time can be easily performed with little effort, even in many different and usually uncertain dynamic environments. This kind of human-like intelligent control idea must not only have the capability to acquire/learn knowledge but also be able to recognize different environments in real time and rapidly decide which measures to take to deal with the current situation. With the advancement of science and technology, the working environment is becoming more complicated, and the system model faces the threat of various unexpected factors, such as system failures, dynamic changes of subsystems, and external disturbances [1]. Inspired by human motion behavior, the development of an advanced control method that recognizes emergencies in real time through autonomous learning and adopts optimal control strategies to ensure the smooth operation of the system has emerged to be a significant yet challenging task.

Over the past few decades, research on learning control (LC) systems, in which the controller is designed to estimate/learn unknown information, has attracted considerable attention. Then, the learned information can be reused as the experience of the controller [2], of which the premise is that true information can be learned. Meanwhile, the pattern recognition method is employed to recognize the current control situation (pattern) of the plant and select the optimal controller to serve [2]. However, the realization of these ideas is a difficult problem because learning in dynamic environments is considered to be the most difficult issue in the fields of adaptive control and LC [3, 4]. Subsequently, by imitating the structure and function of the human brain, neural networks (NNs) and fuzzy systems [5] have attracted

* Corresponding author (email: wangcong@sdu.edu.cn)

considerable research interest because of their powerful learning capabilities. Many approximation-based intelligent control methods have been proposed to solve the tracking control problem of nonlinear systems [6–12], in which NNs are used to approximate/learn the unknown nonlinear dynamics. Moreover, many difficult problems involving NN-based control have been resolved. For example, the "explosion of complexity" issue is overcome by the dynamic surface control technique [13–15], and the existence of implicit ideal control is proven by the implicit function theorem [7, 8, 16]. However, the aforementioned studies only require the convergence of the tracking error to a small residual set. Thus, generally, the transient and steady-state tracking performance cannot be guaranteed, which is a difficult task. To overcome this problem, Ref. [17] proposed an approach called prescribed performance (PP) control [18], which has been recently applied to vehicle active suspension systems [19]. However, the existing intelligent control schemes usually require the control environment to change slowly or remain invariant over time. When the control environments change abruptly and largely, the related control design becomes rather complicated and challenging.

The speed and accuracy of the controller's response to sudden and large changes may be regarded as a measure of intelligence [1]. For those cases where the control situations change from one to another abruptly, traditional adaptive control generally reacts too slowly to those sudden changes, resulting in decreases in transient performance or even instability of the control system [1]. To solve this issue, a representative method called multiple model adaptive control (MMAC) has been proposed in the 1990s, and many interesting results have been reported [1, 20–22]. The basic idea is that there are multiple identification models, including fixed models and adaptive models running in parallel, and the model closest to the current operating regime of the plant according to the identification errors will be determined and used to generate control signals for improved transient performance. However, MMAC can also be categorized as adaptive control, and most of the existing schemes mentioned previously did not explore the learning capability in the adaptive process, thereby lacking the real intelligent capability of knowledge acquisition and reutilization [23]. Therefore, the realization of human-like learning and control capabilities for these methods is still a challenging issue.

Learning capability, that is, acquiring knowledge from a dynamic environment and using learned knowledge to improve control performance, is the core of an intelligent control system [2, 23]. Recently, a mechanism based on adaptive NN control called deterministic learning (DL) theory was proposed by [24, 25]. Accurate learning of the closed-loop dynamics in dynamic environments was obtained, and better control performance was achieved using learned knowledge, which provided a new paradigm for the development of the intelligent control with real learning capability [24, 25]. In addition to the LC problems of nonlinear systems [26–31], some other intelligence-related problems, such as system identification and pattern recognition, have been solved and verified successfully through DL [32–36]. Furthermore, to solve the control problem of uncertain nonlinear systems operating in multiple control situations, a pattern-based control scheme was proposed by [37] for simple affine nonlinear systems and extended to a representative class of pure-feedback systems [38]. Notably, the existing pattern-based control schemes [37, 38] can only guarantee that the tracking error converges to a small residual set but cannot quantitatively calculate the transient and steady-state tracking performance. Moreover, the nth order systems in [38] require $O(n)$ number of NNs to construct controllers and another $O(n)$ number of NNs to construct pattern classifiers (dynamic estimators) for each independent control situation. With the increase in the order of the system and the types of control situations, the number and complexity of NNs to be trained will increase dramatically, resulting in the limited application of pattern-based intelligent control. Therefore, the simple, efficient, and performance-guaranteed design of pattern-based intelligent control is an issue worthy of further investigation.

In this study, we address the problem of pattern-based intelligent control with guaranteed PP for pure-feedback systems operating in multiple control situations. First, the appropriate system transformation technique is introduced to transform the original pure-feedback system into a nonaffine system in normal form. Based on PP, an error transformation technique is employed, and the constrained tracking control problem of the original system is converted into a simple unconstrained stabilization problem. Based on a high gain observer (HGO), a novel adaptive neural control (ANC) scheme is proposed to achieve system stability and prescribed tracking control performance, in which only one NN approximator is used. Because of the simplified control design, the satisfaction of partial persistent excitation (PE) condition of the radial-basis function (RBF) NN can be easily verified, and accurate identification/learning of the implicit unknown dynamics of the transformed system is achieved. By reutilizing the knowledge obtained, a bank of pattern-based candidate controllers for all different control situations is constructed. Second,

to realize the classification of different control situations, an HGO-based NN identifier is developed to learn the transformed system dynamics in all different control situations through DL. With learned knowledge, a set of dynamic estimators is constructed for the classification of different control situations. Third, when the control situation changes abruptly, a set of residuals is obtained by comparing the dynamic estimators with the monitored system; thus, sudden changes can be rapidly recognized based on the minimum residual principle. Finally, based on the recognition results, the correct experience-based controller corresponding to the current control situation is selected to achieve stability and improved control performance.

The main contributions of this work are the following. (1) The proposed HGO-based ANC scheme not only achieves specified transient and steady-state tracking performance, but also realizes accurate identification/learning of the unknown system dynamics. Moreover, only one NN unit is used for each control situation. (2) Learned knowledge can be reutilized to improve the control performance without any further adaptation online, while the prescribed tracking performance can still be guaranteed. (3) In the LC and dynamical pattern recognition processes, the number of NNs to be trained is considerably reduced, and the complexity of control design, recognition, and computation is significantly alleviated. The attraction of the proposed scheme is that autonomous learning, decision-making, and high-performance control are realized in a simple manner, which is consistent with the essential meaning of intelligence (i.e., the capacity to acquire and apply knowledge, see Webster's dictionary), and will provide new ideas for the development of intelligent control methods in dynamic environments.

The remainder of this article is organized as follows. Section 2 reviews the problem formulation and related preliminaries. Two phases of identification/training are implemented in Section 3, and the phases of rapid recognition and control of the changed control situation are presented in Section 4. The simulation studies conducted to verify the method are discussed in Section 5. Finally, Section 6 draws the conclusion.

2 Problem formulation and preliminaries

2.1 Problem formulation

Consider the following nth-order pure-feedback system, which is described as

$$\begin{cases} \dot{x}_i = f_i^k(\bar{x}_i, x_{i+1}),\ 1 \leqslant i \leqslant n-1, \\ \dot{x}_n = f_n^k(\bar{x}_n, u),\ n \geqslant 2, \\ y = x_1, \end{cases} \tag{1}$$

where $\bar{x}_i = [x_1, \ldots, x_i]^{\mathrm{T}} \in \mathbb{R}^i$, $i = 1, 2, \ldots, n$ are the system measurable state vectors, $u \in \mathbb{R}$ and $y \in \mathbb{R}$ are the input and output of the system. We assume that there are $N+1$ different control situations (or patterns), such as possible large changes of the system dynamics/parameters, faults in the subsystems. $f_i^k(\cdot)$ $(i = 1, 2, \ldots, n)$ denote the unknown smooth nonlinear functions of the kth control situation with $k = 0, 1, \ldots, N$.

For system (1), we define

$$g_i^k(\bar{x}_i, x_{i+1}) = \frac{\partial f_i^k(\bar{x}_i, x_{i+1})}{\partial x_{i+1}}, \tag{2}$$

where $i = 1, 2, \ldots, n$ and $x_{n+1} = u$.

Assumption 1 ([8])**.** The signs of the functions $g_i^k(\cdot)$ $(i = 1, 2, \ldots, n)$ are considered known, and there are unknown constants $g_{i\max}^k \geqslant g_{i\min}^k > 0$ such that $g_{i\min}^k \leqslant |g_i^k(\cdot)| \leqslant g_{i\max}^k < \infty$, $\forall (\bar{x}_i, x_{i+1}) \in \Omega_{\bar{x}_{i+1}} \subset \mathbb{R}^{i+1}$, $i = 1, 2, \ldots, n$, $k \in \{0, 1, 2, \ldots, N\}$, where $\Omega_{\bar{x}_{i+1}}$ denotes a compact region.

Assumption 1 means that the defined functions $g_i^k(\cdot)$, $i = 1, 2, \ldots, n$ are strictly either positive or negative. Without loss of generality, it is assumed that all signs are positive. Assumption 1 is reasonable because $g_i^k(\cdot)$ being away from zeros is controllable conditions of system (1), which is made in most of control schemes [39]. It should be emphasized that the upper and lower bounds of $g_i^k(\cdot)$ are only required for analytical purposes, and their true values are not necessarily known.

The desired reference trajectory y_d is generated by

$$\begin{cases} \dot{x}_{d,i} = x_{d,i+1}, & i = 1, \ldots, n-1, \\ \dot{x}_{d,n} = f_d(x_d), & y_d = x_{d,1}, \end{cases} \tag{3}$$

where $x_d = [x_{d,1}, \ldots, x_{d,n}]^{\mathrm{T}} \in \mathbb{R}^n$ is the state vector of the reference system, $y_d \in \mathbb{R}$ is the desired reference output, and $f_d(\cdot)$ denotes a continuous known nonlinear function. It is assumed that $x_{d,i}$ $(i = 1, 2, \ldots, n)$ are bounded and recurrent signals starting from the initial condition $x_d(0)$, and the reference system trajectory is a recurrent orbit expressed as $\varphi_d(x_d(0))$ or φ_d.

Our objective of this study is to develop a pattern-based intelligent control scheme such that all closed-loop signals remain bounded, and the tracking error $e_1(t) = y(t) - y_d(t)$ tends to zero even in the presence of changes in the control situation. More specifically, the tracking error is required to satisfy

$$-\underline{\varpi}\rho(t) \leqslant e_1(t) \leqslant \overline{\varpi}\rho(t), \tag{4}$$

where $\underline{\varpi}$ and $\overline{\varpi}$ are positive constants, $\rho(t)$ is a strictly positive smooth and decreasing performance function. Similar to [17], we choose $\rho(t) = (\rho_0 - \rho_\infty)\mathrm{e}^{-\ell t} + \rho_\infty$, where ρ_0, ρ_∞ and ℓ denote strictly positive constants with ρ_∞ being $\lim_{t\to\infty} \rho(t)$. For any initial condition, $\underline{\varpi}\rho_0$ and $\overline{\varpi}\rho_0$ are appropriately selected such that $\underline{\varpi}\rho_0, \overline{\varpi}\rho_0 > |e_1(0)|$. For the term $\mathrm{e}^{-\ell t}$ in $\rho(t)$, the decreasing rate ℓ of ρ is to prescribe a lower bound on the required speed of convergence of $e_1(t)$. $-\underline{\varpi}\rho(t)$ and $\overline{\varpi}\rho(t)$ are the tracking error's lower and upper bounds at steady state.

The basic framework of the pattern-based intelligent control scheme is shown in Figure 1, which consists of four phases. The first is two offline training/identification phases (see Figures 1(a) and (b)), i.e., the implementation of two levels of knowledge acquisition. The objective is to construct an experience-based controller bank for high-performance control and a set of dynamic estimators for pattern classification. The second is the online recognition phase and control phase (knowledge utilization), i.e., using the candidate controllers and estimators constructed above to design appropriate recognition and controller switching strategies to achieve high-performance control in the case of sudden changes in the control situation (see Figure 1(c)). Next, we seek to address the following intelligence-related issues: (1) how to provide ideal tracking control with PP for each independent control situation (see Section 3); (2) when the control situation changes abruptly, how to rapidly and accurately perceive this change, and adopt appropriate control strategies (see Section 4).

2.2 Preliminary knowledge

The output of the RBF networks can be given by

$$f_{nn}(Z) = \sum_{i=1}^{l} w_i s_i(Z) = W^{\mathrm{T}} S(Z), \tag{5}$$

where $Z \in \Omega_Z \subset \mathbb{R}^q$ is the NN input vector, q is the dimension of the NN input, $W = [w_1, w_2, \ldots, w_l]^{\mathrm{T}} \in \mathbb{R}^l$ denotes the weight vector, $l > 1$ is the network node number, $S(Z) = [s_1(Z), s_2(Z), \ldots, s_l(Z)]^{\mathrm{T}} \in \mathbb{R}^l$ is the vector of the RBF. $s_i(Z)$ is chosen as the commonly used Gaussian function described by $s_i(Z) = \exp[-(Z - \xi_i)^{\mathrm{T}}(Z - \xi_i)/\eta_i^2], i = 1, \ldots, l$, where $\xi_i = [\xi_{i1}, \xi_{i2}, \ldots, \xi_{iq}]^{\mathrm{T}}$ denotes the center of the receptive field, and η_i denotes the Gaussian function's width. As shown in [40] that for any continuous function $f(Z)$ over a compact set $\Omega_Z \in \mathbb{R}^q$, there exists an ideal constant weight vector W^* such that $f(Z)$ can be approximated by NN to any arbitrary accuracy κ^*: $f(Z) = W^{*\mathrm{T}} S(Z) + \kappa(Z), \forall Z \in \Omega_Z \in \mathbb{R}^q$, where $\kappa(Z)$ represents the approximation error with $|\kappa(Z)| \leqslant \kappa^*$.

In [24], the localized RBF networks possess the spatially localized learning abilities of representation, storage, and adaptation. For any bounded trajectory $Z(t)$ over the compact set Ω_Z, $f(Z)$ can be approximated by using only a limited number of neurons, which are located in a local area close to the trajectory, and we obtain

$$f(Z) = W_\zeta^{*\mathrm{T}} S_\zeta(Z) + \kappa_\zeta,$$

where $S_\zeta(Z) = [s_{j_1}(Z), \ldots, s_{j_\zeta}(Z)]^{\mathrm{T}} \in \mathbb{R}^{l_\zeta}$ represents the regression subvector of $S(Z)$, $l_\zeta < l$, $W_\zeta^* = [w_{j_1}^*, \ldots, w_{j_\zeta}^*]^{\mathrm{T}}$ is the corresponding ideal constant weight vector, κ_ζ is approximation error with $||\kappa_\zeta| - |\kappa||$ being small.

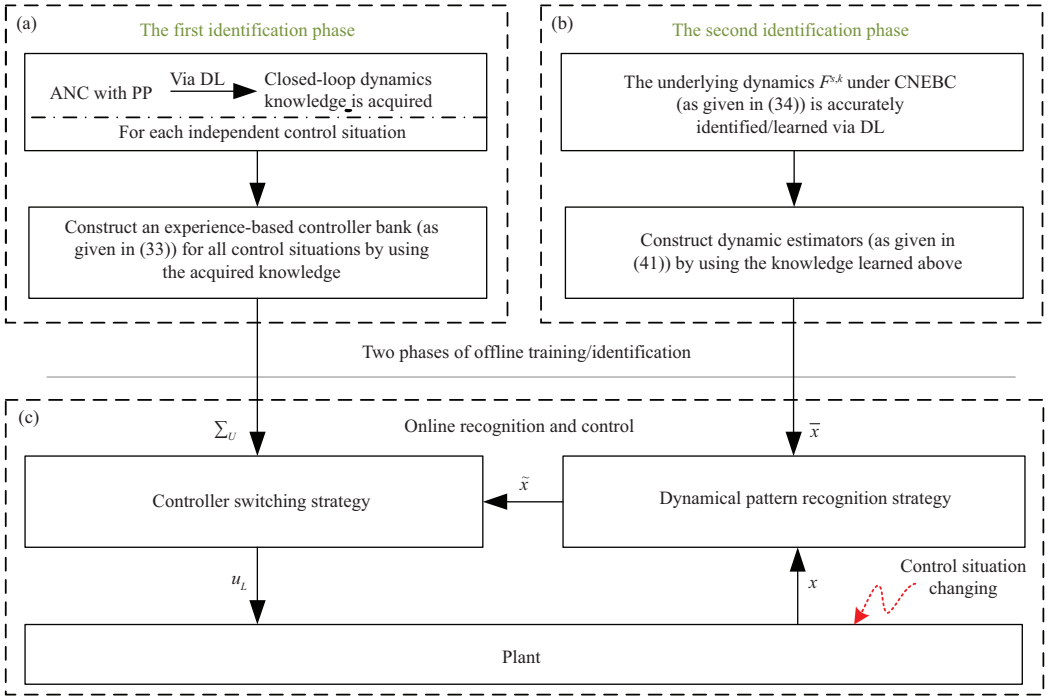

Figure 1 (Color online) Schematic diagram of the pattern-based intelligent control. (a) The first offline training phase; (b) the second offline training phase; (c) online recognition and control when the control situation changes.

Based on the results in [41] about the PE property of the RBF NNs, Wang et al. [24,25] proposed that for a localized RBF NN $W_\zeta^{\mathrm{T}} S_\zeta(Z)$ whose centers are placed on a regular lattice, nearly any recurrent trajectory $Z(t)$ can lead to satisfying the PE condition of $S_\zeta(Z)$, and it is a key factor that enables the true learning capability of the RBF networks to be realized.

3 Offline training/identification phase

In this section, two phases of offline training/identification are first implemented for the pattern-based intelligent control scheme. The objective is to construct a family of candidate experience-based controllers and a bank of dynamic estimators for the $N+1$ different control situations by using the knowledge learned in the two accurate identification phases, respectively.

3.1 The first identification phase—controller design

In the first identification/training phase, for each independent control situation, a novel adaptive neural controller is first designed to achieve convergence of tracking error with PP, and the real learning ability is further achieved in the stable control process via DL. Then, using the knowledge learned in different control situations, a pattern-based candidate controller bank is constructed.

3.1.1 *Constrained error transformation*

In order to achieve the constrained error $e_1(t)$, a performance transformation technique is introduced to convert the original constrained tracking error into a new unconstrained error $\zeta_1(t)$ [17]. We define

$$e_1(t) = \rho(t)\Upsilon(\zeta_1(t)), \tag{6}$$

where $\zeta_1(t)$ is the newly defined transformed error, $\Upsilon(\zeta_1(t))$ is a smooth and increasing invertible function satisfying

$$\begin{cases} \lim_{\zeta_1 \to +\infty} \Upsilon(\zeta_1(t)) = \overline{\varpi}, \\ \lim_{\zeta_1 \to -\infty} \Upsilon(\zeta_1(t)) = -\underline{\varpi}. \end{cases} \tag{7}$$

In this study, we select the transformed function $\Upsilon(\zeta_1(t))$ as

$$\Upsilon(\zeta_1(t)) = \frac{\overline{\varpi}\mathrm{e}^{\zeta_1(t)} - \underline{\varpi}\mathrm{e}^{-\zeta_1(t)}}{\mathrm{e}^{\zeta_1(t)} + \mathrm{e}^{-\zeta_1(t)}}. \tag{8}$$

Furthermore, according to (6) and (8), the unconstrained tracking error can be obtained in the following form:

$$\zeta_1 = \Upsilon^{-1}(e_1(t)/\rho(t)) = \frac{1}{2}\ln\frac{\underline{\varpi} + e_1(t)/\rho(t)}{\overline{\varpi} - e_1(t)/\rho(t)}. \tag{9}$$

Then, the derivative of the unconstrained error is

$$\dot{\zeta}_1 = \varrho\left(\dot{e}_1 - \dot{\rho}(t)/\rho(t)e_1\right), \tag{10}$$

where $\varrho = 1/2\rho(t)(1/(e_1(t)/\rho(t)+\underline{\varpi}) - 1/(e_1(t)/\rho(t)-\overline{\varpi}))$. According to (4), we can conclude that $\varrho > 0$. Notice that from (7) we can see that the inequality $-\underline{\varpi} < \Upsilon(\zeta_1) < \overline{\varpi}$ holds, and by combining (9) we can obtain (4), which means that the tracking error constraints are guaranteed. Subsequently, our objective is to construct an appropriate controller to guarantee that the unconstrained error ζ_1 converges to the vicinity around zero for system (1) operating in different control situations.

3.1.2 *Pattern-based controller*

In order to circumvent the complexity of traditional backstepping control design, in which n NN approximators are generally used for the nth order nonaffine system (1), an appropriate system transformation is implemented to transform the original system (1) into a normal nonlinear system [42]. Let $\hbar_1 = x_1 := Q_1^k(x_1)$, $\hbar_2 = \dot{\hbar}_1 = f_1^k(\bar{x}_2) := Q_2^k(\bar{x}_2)$, and $\hbar_i = \dot{\hbar}_{i-1} := Q_i^k(\bar{x}_i)$ $(i = 3, \ldots, n)$. Then, the original pure-feedback system (1) can be transformed into the following form:

$$\begin{cases} \dot{\hbar}_i = \hbar_{i+1}, & 1 \leqslant i \leqslant n-1, \\ \dot{\hbar}_n = F^k(\bar{x}_n, u), & n \geqslant 2, \\ y = \hbar_1, \end{cases} \tag{11}$$

where

$$F^k(\bar{x}_n, u) = \sum_{j=1}^{n-1} \frac{\partial Q_n^k(\bar{x}_n)}{\partial x_j} f_j^k(\bar{x}_{j+1}) + \frac{\partial Q_n^k(\bar{x}_n)}{\partial x_n} f_n^k(\bar{x}_n, u) \tag{12}$$

with $\partial Q_i^k(\bar{x}_i)/\partial x_i = \prod_{j=1}^{i-1} g_j^k(\bar{x}_{j+1})$. Based on (2), $\partial F^k(\bar{x}_n, u)/\partial u = \partial Q_n^k(\bar{x}_n)/\partial x_n \partial f_n^k(\bar{x}_n, u)/\partial u$ holds. Let $G^k(\bar{x}_n, u) = \partial F^k(\bar{x}_n, u)/\partial u$. By combining Assumption 1, we have $G_{\min}^k \leqslant G^k(\bar{x}_n, u) \leqslant G_{\max}^k$ with $G_{\min}^k = \prod_{j=1}^n g_{j\min}^k$, $G_{\max}^k = \prod_{j=1}^n g_{j\max}^k$. For more details, please refer to [42].

From the transformation process, we can easily find that the new states $\hbar_i$ $(i = 2, 3, \ldots, n)$ are unavailable for controller design since the composition of state $\hbar_i$ involves the unknown functions f_j^k $(\bar{x}_{j+1})$ $(j = 1, 2, \ldots, n)$, and the only available state for measurement is the output signal $\hbar_1$. $F^k(\bar{x}_n, u)$ $(k \in 0, 1, 2, \ldots, N)$ as given in (12) denotes the transformed unknown nonaffine function. To cope with the unmeasurable issue of the new states $\hbar_i$ $(i = 2, \ldots, n)$ [43], we consider the following observer as described in Lemma 1.

Lemma 1. Suppose the output $y(t)$ and its first n derivatives are all bounded. Consider the linear system in the following form:

$$\begin{cases} r\dot{\varsigma}_i = \varsigma_{i+1}, & 1 \leqslant i \leqslant n-1, \\ r\dot{\varsigma}_n = -h_1\varsigma_n - h_2\varsigma_{n-1} - \cdots - \varsigma_1 + y(t), & n \geqslant 2, \end{cases} \tag{13}$$

where $r > 0$ is any small constant and the parameters h_i $(i = 1, 2, \ldots, n-1)$ are selected such that the polynomial $s^n + h_1 s^{n-1} + \cdots + h_{n-1}s + 1$ is Hurwitz. Thus, there exist constants $H_j > 0$ $(j = 2, 3, \ldots, n)$ and t^*, for all $t > t^*$, such that

$$\frac{\varsigma_{j+1}}{r^j} - y^{(j)} = -r\phi^{(j+1)}, \quad \left|\phi^{(j+1)}\right| \leqslant H_{j+1}, \ j = 1, 2, \ldots, n-1,$$

where $\phi = \varsigma_n + h_1\varsigma_{n-1} + \cdots + h_{n-1}\varsigma_1$ and $\phi^{(j)}$ represents ϕ's jth derivative. For detailed proof of Lemma 1, please refer to [43].

For ease of design and analysis, vectors $e = \hbar - Y_d = [e_1, e_2, \ldots, e_n]^{\mathrm{T}}$ and $\hat{e} = \hat{\hbar} - Y_d = [\hat{e}_1, \hat{e}_2, \ldots, \hat{e}_n]^{\mathrm{T}}$ are defined, where $\hat{\hbar} = [\varsigma_1, \varsigma_2/r, \ldots, \varsigma_n/r^{n-1}]^{\mathrm{T}}$, $\hbar = [\hbar_1, \hbar_2, \ldots, \hbar_n]^{\mathrm{T}}$, and $Y_d = [y_d, \dot{y}_d, \ldots, y_d^{(n-1)}]^{\mathrm{T}}$. Then, we obtain

$$\tilde{e} = \hat{e} - e = [\tilde{e}_1, \tilde{e}_2, \ldots, \tilde{e}_n]^{\mathrm{T}} = \left[0, \frac{\varsigma_2}{r} - \hbar_2, \ldots, \frac{\varsigma_n}{r^{n-1}} - \hbar_n\right]^{\mathrm{T}}. \tag{14}$$

Based on the observer (13) and backstepping technique, the control design for the transformed system (11) is as follows.

Step 1. By combining (10) and (14), the derivative of the unconstrained error ζ_1 can be expressed as

$$\dot{\zeta}_1 = \varrho\left(\hbar_2 - \dot{y}_d - \dot{\rho}(t)/\rho(t)e_1\right). \tag{15}$$

We define $\zeta_i = \varsigma_i/r^{i-1} - \alpha_{if}$ $(i = 2, 3, \ldots, n)$, where α_{if} is the first-order filtered output of virtual control α_i as given below. From (14), we have $\tilde{e}_2 = \varsigma_2/r - \hbar_2$. Notice that $\zeta_2 = \varsigma_2/r - \alpha_{2f}$, Eq. (15) can be rewritten as

$$\dot{\zeta}_1 = \varrho\left(\zeta_2 - \dot{y}_d - \tilde{e}_2 + \alpha_{2f} - \dot{\rho}(t)/\rho(t)e_1\right). \tag{16}$$

Then, the following virtual control law is proposed as

$$\alpha_2 = -c_1\zeta_1 + \dot{\rho}(t)/\rho(t)e_1 + \dot{y}_d, \tag{17}$$

where $c_1 > 0$ denotes a design constant. Then, a new state variable α_{if} is introduced; i.e., virtual control α_i is passed through a first-order filter with the time constant τ_i [13]. We have

$$\tau_i\dot{\alpha}_{if} + \alpha_{if} = \alpha_i,\ i = 2, 3, \ldots, n, \quad \alpha_{if}(0) = \alpha_i(0). \tag{18}$$

For the convenience of the first-order filter implementation, we define $y_{i+1} = \alpha_{(i+1)f} - \alpha_{i+1}, i = 1, 2, \ldots, n-1$. Notice that $\dot{\alpha}_{(i+1)f} = -y_{i+1}/\tau_{i+1}$, and then

$$\begin{aligned}\dot{y}_{i+1} &= -\frac{y_{i+1}}{\tau_{i+1}} + c_i\dot{\zeta}_i - \ddot{\alpha}_{if} + \dot{\zeta}_{i-1}\\ &= -\frac{y_{i+1}}{\tau_{i+1}} + \Phi_{i+1}(\zeta_1, \ldots, \zeta_{i+1}, y_2, \ldots, y_{i+1}, y_d, \dot{y}_d, \ddot{y}_d),\end{aligned} \tag{19}$$

where $i = 1, 2, \ldots, n-1$, $\dot{\alpha}_{1f} = \dot{y}_d$, $\zeta_0 = 0$, and Φ_{i+1} is a continuous function. According to the analysis made in [13], there exists a maximum M_{i+1} that satisfies $|\Phi_{i+1}| \leqslant M_{i+1}$ (please refer to [13] for details). Then, we have

$$\dot{\zeta}_1 = \varrho\left(-c_1\zeta_1 + \zeta_2 - \tilde{e}_2 + y_2\right). \tag{20}$$

Step i **(**$2 \leqslant i \leqslant n-1$**).** According to the definition in step 1, we know $\zeta_i = \varsigma_i/r^{i-1} - \alpha_{if}$. By combining (13), we have

$$\dot{\zeta}_i = \varsigma_{i+1}/r^i - \dot{\alpha}_{if}. \tag{21}$$

Then, we propose the virtual control laws α_{i+1} as shown below:

$$\alpha_{i+1} = -c_i\zeta_i + \dot{\alpha}_{if} - \zeta_{i-1}, \tag{22}$$

where c_i denotes the positive design constant. Then, by combining (22) and $\zeta_{i+1} = \varsigma_{i+1}/r^i - \alpha_{(i+1)f}$, Eq. (21) can be rewritten as

$$\dot{\zeta}_i = -c_i\zeta_i + y_{i+1} + \zeta_{i+1} - \zeta_{i-1}. \tag{23}$$

Step n**.** Notice that $\zeta_n = \varsigma_n/r^{n-1} - \alpha_{nf}$ and $\varsigma_n/r^{n-1} - y^{(n-1)} = -r\phi^{(n)}$ (as given in Lemma 1). We have $\zeta_n = y^{(n-1)} - r\phi^{(n)} - \alpha_{nf}$. According to (11), it follows that $z_n = y^{(n-1)}$; then we have

$$\dot{\zeta}_n = F^k(\bar{x}_n, u) - r\phi^{(n+1)} - \dot{\alpha}_{nf}. \tag{24}$$

Next, letting $\upsilon = -\dot{\alpha}_{nf} + \zeta_{n-1}$, we know $\partial\upsilon/\partial u = 0$. Based on (12), we obtain $\partial\left[F^k(\bar{x}_n, u) + \upsilon\right]/\partial u = G^k(\bar{x}_n, u) \geqslant G^k_{\min} > 0, k \in \{0, 1, 2, \ldots, N\}$. Utilizing the implicit function theorem [7], there exists a smooth implicit function $u^{*k}(\bar{x}_n, \upsilon)$ that makes $F^k(\bar{x}_n, u^{*k}) + \upsilon = 0$. Utilizing the mean value theorem [44], we have

$$F^k(\bar{x}_n, u^k) - F^k(\bar{x}_n, u^{*k}) = G^k_\chi(u^k - u^{*k}), \tag{25}$$

where $G^k_\chi = G^k(\bar{x}_n, u^k_\chi)$, $u^k_\chi = \chi u^k + (1-\chi)u^{*k}$ with $0 < \chi < 1$. Hence, by combining Assumption 2 and (12), we obtain $G^k_{\min} \leqslant G^k_\chi \leqslant G^k_{\max}$. According to (24) and (25), we have

$$\dot{\zeta}_n = G^k_\chi(u^k - u^{*k}) - r\phi^{(n+1)} - \zeta_{n-1}. \tag{26}$$

Then, consider an RBF network approximation:

$$u^{*k}(Z) = W^{*k^{\mathrm{T}}}_U S(Z) + \kappa^k, \tag{27}$$

where $Z = [\bar{x}^{\mathrm{T}}_n, \upsilon]^{\mathrm{T}} \in \mathbb{R}^{n+1}$, κ^k is the approximation error satisfying $|\kappa^k| \leqslant \kappa^{*k}$, and W^*_U denotes the optimal constant weight vector. Then, we propose the actual control law u^k as

$$u^k = -c_n\zeta_n + \hat{W}^{k^{\mathrm{T}}}_U S(Z), \tag{28}$$

where u^k denotes the adaptive neural control law corresponding to the kth control situation, c_n denotes a positive design constant, $\hat{W}^k_F$ denotes the estimate of W^{*k}_U, and $\tilde{W}^k_U = \hat{W}^k_U - W^{*k}_U$ denotes the estimation error. The update law of neural weight $\hat{W}^k_U$ is determined as

$$\dot{\hat{W}}^k_U = -\Gamma^k_U[S(Z)\zeta_n + \sigma^k_U\hat{W}^k_U], \tag{29}$$

where $k \in \{0, 1, 2, \ldots, N\}$, $\Gamma^k_U = \Gamma^{k^{\mathrm{T}}}_U$ is the positive adaptation gain matrix, $\sigma^k_U > 0$ denotes a design constant. Next, by combining (27) and (28), Eq. (26) can be rewritten as

$$\dot{\zeta}_n = G^k_\chi(-c_n\zeta_n + \tilde{W}^{k^{\mathrm{T}}}_U S(Z) - \kappa^k) - r\phi^{(n+1)} - \zeta_{n-1}. \tag{30}$$

Then, the closed-loop stability result and accurate identification are summarized as the following theorem.

Theorem 1. Consider the controlled plant characterized by (1) under Assumption 1, prescribed performance condition (4), reference model (3) and the observer (13), and the actual control law given by (28), and update law (29). Then, for any bounded initial conditions on a compact set Ω_0 satisfying (4), we have that (i) all closed-loop signals remain bounded and the tracking error e_1 described by (4) converges to a small region around zero in a finite time T^k; (ii) locally accurate identification/learning of the transformed implicit desired control dynamics $u^{*k}(\bar{x}_n, \upsilon)$ can be obtained by $\hat{W}^{k^{\mathrm{T}}}_U S(Z)$ and $\bar{W}^{k^{\mathrm{T}}}_U S(Z)$ along the recurrent trajectory $Z(t)$, where

$$\bar{W}^k_U = \mathrm{mean}_{t\in[t^k_a, t^k_b]}\hat{W}^k_U(t) \tag{31}$$

with $t^k_b > t^k_a > T^k$.

Proof. Please see Appendix A.

From the analysis in Appendix A, accurate identification/learning of $u^{*k}(\bar{x}_n, \nu)$ for different control situations is obtained by the constant RBF network $\bar{W}^{k^{\mathrm{T}}}_U S(Z)$, where the knowledge learned from accurate identification can be expressed as: for the experienced reference recurrent trajectory $\varphi_d(x_d(t))$, there are small constants $d^{*k} > 0$ and $\epsilon^{*k} > 0$ $(k = 0, 1, 2, \ldots, N)$ that describe a local region Ω_{φ_d} along $\varphi_d(x_d(t))$, such that

$$\mathrm{dist}\left(\varphi\left(Z\left(t\right)\right)|_{t\geqslant T^k}, \varphi_d\left(x_d\left(t\right)\right)\right) < d^{*k} \Rightarrow \left|\bar{W}^{k^{\mathrm{T}}}_U S\left(Z\right) - u^{*k}(\bar{x}_n, \nu)\right| < \epsilon^{*k}, \tag{32}$$

where ϵ^{*k} is close to κ^{*k}. Once the kth control situation recurs, in other words, when the NN input $Z\left(t\right)$ enters area Ω_{φ_d}, the previously learned constant network $\bar{W}^{k^{\mathrm{T}}}_U S(Z)$ in the kth control situation will provide precise approximation for $u^{*k}(\bar{x}_n, \nu)$. We assume that all the $N+1$ different control situations are trained in the first identification/training phase in advance, based on the adaptive neural controller (28),

and then a bank of candidate pattern-based experienced controller is constructed using the learned constant RBF NNs. Each candidate controller corresponds to a specific type of control situation, which can be described as

$$\Sigma_U = \left\{ u_L^k = -c_n\zeta_n + \bar{W}_U^{k^{\mathrm{T}}} S(Z) | k = 0, 1, 2, \ldots, N \right\}. \tag{33}$$

Under the action of the correct experience-based controller, improved control performance can be obtained for each control situation of plant (1), and a detailed proof of theorem will be given in the last pattern-based control phase.

Here ends the first identification phase, and pattern-based candidate controllers (which are all experience-based controllers) are constructed for each control situation, which will provide a candidate controller bank for the last pattern-based control phase.

Remark 1. For a system that is operating normally, when the control situation changes abruptly, the internal dynamics of the system changes accordingly. How to rapidly and correctly recognize the occurrence and type of the sudden change is a challenging issue. To solve this difficulty, the second phase of identification is introduced in Subsection 3.2, where the current normal experience-based controller (CNEBC) will play an important role in the implementation process.

3.2 The second identification phase

For the controlled plant operating stably with multiple control situations, when the control situation changes, the internal nonlinear dynamics will change accordingly. It is difficult to figure out which part of the nonlinear dynamics has changed since the system dynamics is normally unknown. Benefiting from the candidate controller constructed in the first identification phase as given by (33), in this identification phase, we will identify the underlying system dynamics $f_i^k(\cdot), i = 1, 2, \ldots, n$ of plant (1) under the action of CNEBC. However, from the system transformation (11), it is seen that the nonlinear dynamics $F^k(\bar{x}_n, u)$ contains all the dynamic characteristics of plant (1). Then, only one synthetic nonlinear dynamics $F^k(\bar{x}_n, u)$ needs to be identified for the nth order system (1). Because the newly defined state $\hbar_n$ is not available for measurement, the observer is used again to estimate $\hbar_n$.

We assume that plant (1) is operating normally in the sth control situation (also known as pattern s), and u_L^s as given by (33) denotes the corresponding CNEBC. The transformed system (11) controlled by CNEBC u_L^s in different control situation can be expressed as

$$\begin{cases} \dot{\hbar}_i = \hbar_{i+1}, & 1 \leqslant i \leqslant n-1, \\ \dot{\hbar}_n = F^{s,k}(\bar{x}_n, u_L^s), & n \geqslant 2, \end{cases} \tag{34}$$

where $k = 0, 1, 2, \ldots, N, s \in \{0, 1, 2, \ldots, N\}$.

Assumption 2 ([33, 37])**.** The states of (1) are uniformly bounded when the plant is controlled by CNEBC $u_L^s, s \in \{0, 1, 2, \ldots, N\}$ when operating in the $N+1$ different control situations.

Since the change of control situation can also be regarded as a system failure, and this assumption is a formal one in the literature of fault diagnosis (e.g., [33] and the references therein). The reason for introducing such a uniform boundedness assumption is that for design and analysis of a fault detection and isolation scheme, the system states and controls must be measurable signals and so remain bounded before and after the occurrence of a fault (i.e., before and after the control situation changes).

By recalling the observer (13), we construct the following dynamical RBF NN identifier to learn the synthetic unknown nonlinear dynamics in (34), which is expressed as

$$\dot{\hat{\hbar}}_n = -a^k(\hat{\hbar}_n - \varsigma_n/r^{n-1}) + \hat{W}_F^{s,k^{\mathrm{T}}} S_F(Z_F), \tag{35}$$

where $\hat{\hbar}_n$ denotes the identifier state, ς_n/r^{n-1} is the state of observer (13), a^k denotes a design positive constant, and $\hat{W}_F^{s,k^{\mathrm{T}}} S_F(Z_F)$ is used to approximate $F^{s,k}(\bar{x}_n, u_L^s)$ with the NN input $Z_F = [\bar{x}_n^{\mathrm{T}}, u_L^s]^{\mathrm{T}}$. We consider the adaptive update law as shown below:

$$\dot{\hat{W}}_F^{s,k} = \Gamma_F^k[-S_F(Z_F)\tilde{\hbar}_n - \sigma_F^k \hat{W}_F^{s,k}], \tag{36}$$

where $\tilde{\hbar}_n = \hat{\hbar}_n - \varsigma_n/r^{n-1}$, $\Gamma_F^k = \Gamma_F^{k^{\mathrm{T}}} > 0$, and $\sigma_F^k > 0$ are design constants. Let $\tilde{W}_F^{s,k} = \hat{W}_F^{s,k} - W_F^{*s,k}$, where $W_F^{*s,k}$ denotes the optimal constant neural weight vector.

From Lemma (1) and the definition of $\hbar_n$, we have $\varsigma_n/r^{n-1} - \hbar_n = -r\phi^{(n)}$. Utilizing the local approximation property of RBF NN, the entire identification error system consisting of system (34), dynamical identifier (35), observer (13), and neural update law (36) can be represented as

$$\begin{bmatrix} \dot{\tilde{\hbar}}_n \\ \dot{\tilde{W}}^{s,k}_{F\zeta} \end{bmatrix} = \left[\begin{array}{c|c} -a^k & S^{\mathrm{T}}_{F\zeta}(Z_F) \\ \hline -\Gamma^k_{F\zeta} S_{F\zeta}(Z_F) & 0 \end{array}\right] \begin{bmatrix} \tilde{\hbar}_n \\ \tilde{W}^{s,k}_{F\zeta} \end{bmatrix} + \begin{bmatrix} \kappa^{s,k}_{\zeta} + r\phi^{(n+1)} \\ -\sigma^k_F \Gamma^k_{F\zeta} \hat{W}^{s,k}_{F\zeta} \end{bmatrix}, \tag{37}$$

and

$$\dot{\tilde{W}}^{s,k}_{F\bar{\zeta}} = -\Gamma^k_{F\bar{\zeta}} S_{F\bar{\zeta}}(Z_F)\tilde{\hbar}_n - \sigma^k_F \Gamma^k_{F\bar{\zeta}} \hat{W}^{s,k}_{F\bar{\zeta}}, \tag{38}$$

where $\kappa^{s,k}_{\zeta} = \kappa^{s,k} - \tilde{W}^{s,k^{\mathrm{T}}}_{F\bar{\zeta}} S_{F\bar{\zeta}}(Z_F)$, $\kappa^{s,k} = F^{s,k}(Z_F) - W^{*s,k^{\mathrm{T}}}_F S_F(Z_F)$. $(\cdot)_{i\zeta}$ and $(\cdot)_{i\bar{\zeta}}$ represent the regions that are near and far away from the trajectory Z_F, respectively. Based on the analysis in Theorem 1, we know that the states $x_i, i = 1, 2, \ldots, n$ are recurrent signals. By combining Assumption 2, x_i will also be a kind of recurrent signal. Furthermore, notice that u^s_L (as given by (33)) is a function of x_i and x_d, which are all recurrent signals; thus, u^s_L is also a recurrent signal. Therefore, the NN input $Z_F = [\bar{x}^{\mathrm{T}}_n, u^s_L]^{\mathrm{T}}$ follows the recurrent trajectory and the partial PE condition of $S_{F\zeta}(Z_F)$ is further established based on the results in [24]. According to the stability results in [45], the exponential convergence of $\tilde{\hbar}_n$ and $\tilde{W}^{s,k}_{F\zeta}$ of the nominal part of (37) can be obtained. Notice that $\phi^{(n+1)} \leqslant H_{n+1}$; thus, both $|\kappa^{s,k}_{\zeta} + r\phi^{(n+1)}|$ and $\|\sigma^k_F \Gamma^k_{F\zeta} \hat{W}^{s,k}_{F\zeta}\|$ can be small values by choosing enough small r and σ^k_F. Based on Lemma 4.6 in [46], $\tilde{W}^{s,k}_{F\zeta}$ will exponentially converge to a small region around zero with the convergence area being determined by $|\kappa^{s,k}_{\zeta} + r\phi^{(n+1)}|$ and $\|\sigma^k_F \Gamma^k_{F\zeta} \hat{W}^{s,k}_{F\zeta}\|$, which implies that $\hat{W}^{s,k}_{F\zeta}$ can converge to a small region of $W^{*s,k}_{F\zeta}$. Then, we can conclude that, along the trajectory Z_F, $F^{s,k}(\bar{x}_n, u^s_L)$ can be accurately identified by $\hat{W}^{s,k^{\mathrm{T}}}_{F\zeta} S_{F\zeta}(Z_F)$ and $\bar{W}^{s,k^{\mathrm{T}}}_F S_F(Z_F)$, which can be expressed as

$$F^{s,k}(\bar{x}_n, u^s_L) = \hat{W}^{s,k^{\mathrm{T}}}_{F\zeta} S_{F\zeta}(Z_F) + \kappa^{s,k}_{F\zeta} = \bar{W}^{s,k^{\mathrm{T}}}_F S_F(Z_F) + \bar{\kappa}^{s,k}_F, \tag{39}$$

where $\kappa^{s,k}_{F\zeta}$ and $\bar{\kappa}^{s,k}_F$ are close to $\kappa^{*s,k}_F$, and $\bar{W}^{s,k}_F = \mathrm{mean}_{t\in[t'_a,t'_b]} \hat{W}^{s,k}_F(t)$ denotes a constant neural weight vector learned in the second identification phase with $t'_b > t'_a > 0$ representing a time interval after the transient process. Similar to (32), for the experienced recurrent trajectory Z^k_F, there are small constants $d^{*s,k}_F > 0$ and $\epsilon^{*s,k}_F > 0$ that describe a local region Ω_{F,Z^k_F} along Z^k_F, such that

$$\mathrm{dist}((\bar{x}_n, u^s_L), Z^k_F(t)) < d^{*s,k}_F \Rightarrow \left|\bar{W}^{s,k^{\mathrm{T}}}_F S_F(Z_F) - F^{s,k}(\bar{x}_n, u^s_L)\right| < \epsilon^{*s,k}_F, \tag{40}$$

where $\epsilon^{*s,k}_F$ denotes the NN identification error and $\epsilon^{*s,k}_F$ is close to $\kappa^{*s,k}_F$. That is, under the action of CNEBC u^s_L, the unknown synthetic nonlinear dynamics $F^{s,k}(\bar{x}_n, u^s_L)$ corresponding to the kth control situation can be represented by the constant NN $\bar{W}^{s,k^{\mathrm{T}}}_F S_F(Z_F)$ with guaranteed approximation accuracy. Then, a set of dynamic estimators is constructed using $\bar{W}^{s,k^{\mathrm{T}}}_F S_F(Z_F)$ as

$$\dot{\bar{\hbar}}^k_n = -b(\bar{\hbar}^k_n - \varsigma_n/r^{n-1}) + \bar{W}^{s,k^{\mathrm{T}}}_F S_F(Z_F), \tag{41}$$

where $\bar{\hbar}^k_n$ $(k = 0, 1, 2, \ldots, N)$ denotes the state of (41), $b > 0$ is a design constant, and $\bar{W}^{s,k^{\mathrm{T}}}_F S_F(Z_F)$ is the constant NN learned in the previous training phase. With the dynamic model (41), which can be regarded as training patterns, rapid recognition of change in control situation for plant (1) will be achieved in Section 4.

4 Online recognition and control phases

Now let us assume that the controlled plant (1) is currently operating stably in pattern 0 and is controlled by u^0_L (as given by (33), where $s = 0$). Due to some unknown factors, the control situation of plant (1) changes to the jth control situation at an unknown instant. Then, how to rapidly recognize the occurrence and type of changes and achieve precise control is a very important as well as challenging issue. Based on the dynamic model (41) constructed in Subsection 3.2 and the candidate experience-based controllers as given by (33), a novel rapid recognition and control scheme will be proposed in Subsections 4.1 and 4.2, and the block diagram of the overall pattern-based control is shown in Figure 2.

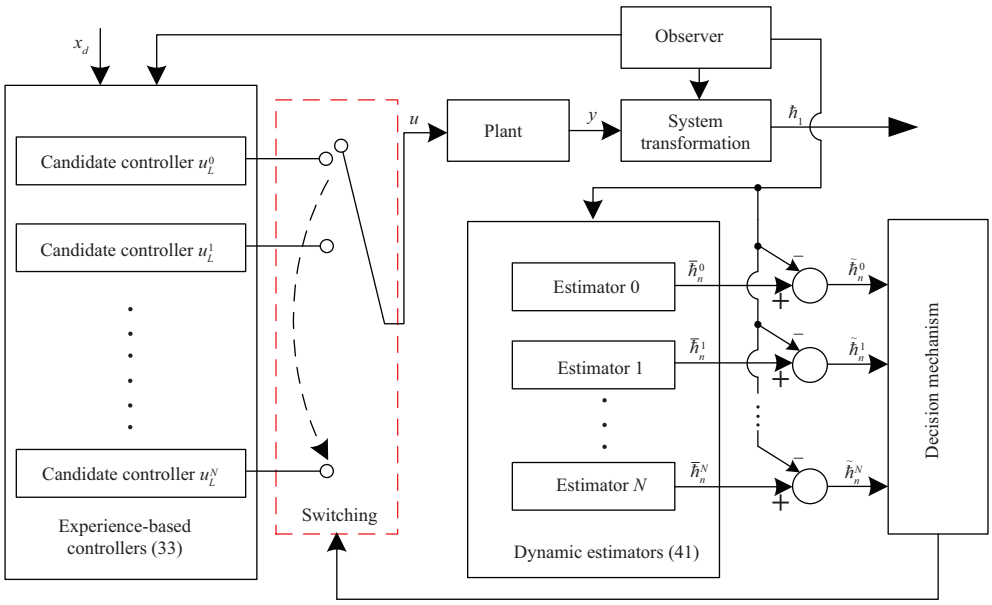

Figure 2 (Color online) Block diagram of pattern-based control.

4.1 Rapid recognition scheme

If the control situation of plant (1) changes from the 0th to the jth ($j \in \{0,1,\ldots,N\}$), the synthetic dynamics $F^0(\bar{x}_n, u_L^0)$ changes to $F^j(\bar{x}_n, u_L^0)$ accordingly, and the following assumption is introduced.

Assumption 3 ([33,37])**.** For the controlled system under u_L^s as given by (33), $s \in \{0,1,\ldots,N\}$, the difference in dynamics between different control situations satisfies $|F^{s,k}(\bar{x}_n, u_L^s) - F^{s,j}(\bar{x}_n, u_L^s)| \geqslant 2\mu_F^{s,k}$, $k,j \in \{0,1,\ldots,N\}$ and $k \neq j$, where $\mu_F^{s,k} > \kappa_F^{*s,k}$ is a positive constant with $\kappa_F^{*s,k}$ being the ideal identification error.

In dynamical pattern recognition based on NN [32], Assumption 3 is reasonable, because even ideal NN identification has approximation errors. If the system dynamic difference is less than the approximation error, then the NN-based pattern recognition will not be guaranteed, which is a sufficient condition for effective recognition. We refer the interested readers to Lemma 1 in [33] for details.

Then, by comparing the dynamics of the nth subsystem of (34) under u_L^0 with the $N+1$ dynamic estimators as given by (41) (where $s=0$), and combining $\varsigma_n/r^{n-1} - \hbar_n = -r\phi^{(n)}$, the following recognition residual system is obtained as

$$\dot{\tilde{\hbar}}_n^k = -b\tilde{\hbar}_n^k + \bar{W}_F^{0,k^{\mathrm{T}}} S_F(Z_F) - F^{0,j}(\bar{x}_n, u_L^0) + r\phi^{(n+1)}, \tag{42}$$

where $k = 0,1,\ldots,N$, $\tilde{\hbar}_n^k = \bar{\hbar}_n^k - \varsigma_n/r^{n-1}$, $|\bar{W}_F^{0,k^{\mathrm{T}}} S_F(Z_F) - F^{0,j}(\bar{x}_n, u_L^0)|$ denotes the dynamic difference between the controlled system and the kth dynamic model, and $j \in \{0,1,\ldots,N\}$ denotes that the controlled system is operating in the jth control situation. Similar to the analysis of Theorem 2 in [32], by selecting enough small r, the synchronization residual $\tilde{\hbar}^k$ will exponentially converge to a small region around zero with the size of the region being determined by the difference between the system dynamics of the current control situation and the dynamic estimators.

Based on [32,33], the L_1 norm of $\tilde{\hbar}^k$ is used to measure the difference between the system dynamics of the current control situation (34) and the dynamic model (41) as

$$\|\tilde{\hbar}_n^k(t)\|_1 = \frac{1}{T_0}\int_{t-T_0}^{t} |\tilde{\hbar}_n^k(\imath)|\mathrm{d}\imath, \quad t \geqslant T_0, \tag{43}$$

where $k = 0,1,\ldots,N$, $0 < T_0 \leqslant T$, and T denotes the period of the reference trajectory, with which the rapid recognition can be realized and Theorem 2 is concluded as follows.

Theorem 2. Considering the recognition residual system (42) consisting of system (34) in the jth control situation, observer (13), dynamic estimators (41) with Assumptions 2 and 3, we have that rapid recognition of the recurring jth control situation can be realized by comparing the average L_1 norm of the recognition residual (43).

To detect the change of the control situation of plant (11), through the differences between system dynamics of (34) and a series of dynamic estimators, the occurrence and type of the change in control situation can be rapidly recognized. To be more specific, if the control situation of the controlled system (11) does not change, i.e., Eq. (11) is operating normally in pattern 0, the dynamic model representing pattern 0 matches the controlled system (11); thus, the corresponding recognition residual $\|\tilde{\hbar}_n^0(t)\|_1$ will be the smallest one among all the recognition residuals $\|\tilde{\hbar}_n^k(t)\|_1$ $(k=0,1,\ldots,N)$. If the control situation change to the jth ($j\in\{1,2,\ldots,N\}$) one at time t_{0_j}, the previous learned constant RBF NN $\bar{W}_F^{0,j^{\mathrm{T}}}S_F(Z_F)$ embedded in the dynamic model j will quickly provide an accurate approximation for $F^{0,j}(\bar{x}_n,u_L^0)$; thus, the corresponding recognition residual $\|\tilde{\hbar}_n^j(t)\|_1$ will decrease, while the others including $\|\tilde{\hbar}_n^0(t)\|_1$ will be larger than $\|\tilde{\hbar}_n^j(t)\|_1$, which implies that the recurring jth control situation can be rapidly recognized at time $t_{0_{j'}}$. Thereafter, based on the recognition results, the correct experienced candidate controller u^j will be quickly selected to control the current system for improved control performance. For detailed proof of Theorem 2, we refer the readers to [32,33].

Remark 2. It is noted that the dynamic model (41) is actually a representation of the unknown dynamics of system (34). Therefore, when the control situation of the controlled plant changes, accurate recognition can be realized by comparing the dynamic matching between the current system dynamics and the set of dynamic estimators (as given by (41)). Because no further online parameter estimation is required, the recognition process can be done rapidly.

4.2 Pattern-based control

Following Subsection 4.1, the controlled system is initially ($t\geqslant t_0$) operating stably in pattern 0 under CNEBC u_L^0 (as given by (33)). Due to some unknown factors, the control situation changes from the 0th to the jth ($j\in\{1,2,\ldots,N\}$) at time t_{0_j}, the internal system dynamics will change accordingly, and the current (changed) system is still controlled by u_L^0 before the change is recognized. Based on the rapid recognition scheme proposed in Subsection 4.1, the changed jth control situation can be recognized rapidly at time $t_{0_{j'}}$. Then, based on the recognition result, the correct candidate experienced controller u_L^j is quickly selected to control the current controlled system for improved control performance. However, when u_L^j is selected at time $t_{0_{j'}}$, the initial neural input of the constant RBF NN $\bar{W}_U^{j^{\mathrm{T}}}S(Z)$ embedded in u^j might be beyond the region Ω_{φ_d} (as given by (32)); thus, a high gain experienced controller $u_L^{j'}$ is put into use first for a short period of time $[t_{0_{j'}},t_{0_{j''}}]$, after then, u_L^j is selected. In summary, the pattern-based control process for the controlled system can be described as

$$\begin{cases}\dot{\hbar}_i=\hbar_{i+1}, & 1\leqslant i\leqslant n-1,\\ \dot{\hbar}_n=F^0(\bar{x}_n,u_L^0), & \text{if}\ \ t_0\leqslant t<t_{0_j},\\ \dot{\hbar}_i=\hbar_{i+1}, & 1\leqslant i\leqslant n-1,\\ \dot{\hbar}_n=F^j(\bar{x}_n,u_L^0), & \text{if}\ \ t_{0_j}\leqslant t<t_{0_{j'}},\\ \dot{\hbar}_i=\hbar_{i+1}, & 1\leqslant i\leqslant n-1,\\ \dot{\hbar}_n=F^j(\bar{x}_n,u_L^{j'}), & \text{if}\ \ t_{0_{j'}}\leqslant t<t_{0_{j''}},\\ \dot{\hbar}_i=\hbar_{i+1}, & 1\leqslant i\leqslant n-1,\\ \dot{\hbar}_n=F^j(\bar{x}_n,u_L^j), & \text{if}\ \ t_{0_{j''}}\leqslant t<t_j,\end{cases}\tag{44}$$

where the corresponding candidate experienced controllers are given by

$$\begin{cases}u_L^0=-c_n\zeta_n+\bar{W}_U^{0^{\mathrm{T}}}S(Z), & \text{if}\ \ t_0\leqslant t<t_{0_{j'}},\\ u_L^{j'}=-c_n^h\zeta_n+\bar{W}_U^{j^{\mathrm{T}}}S(Z), & \text{if}\ \ t_{0_{j'}}\leqslant t<t_{0_{j''}},\\ u_L^j=-c_n\zeta_n+\bar{W}_U^{j^{\mathrm{T}}}S(Z), & \text{if}\ \ t_{0_{j''}}\leqslant t<t_j,\end{cases}\tag{45}$$

where c_n^h denotes the high control gain satisfying $c_n^h\gg c_n$.

By combining the constructed candidate experienced controllers, as given by (33), and the proposed rapid recognition scheme, the controlled system (1) will keep stable with prescribed tracking performance as described by (4), even in the presence of changes in control situation. Theorem 3 is concluded as follows.

Theorem 3. Consider the pattern-based closed-loop control system consisting of controlled system (44), prescribed performance condition (4), reference model (3), observer (13), candidate experienced controllers (45) with the virtual control laws (17) and (22). For the same recurrent trajectory $\varphi_d(0)$ and initial condition $x(0)$ as in Theorem 1, by choosing the appropriate parameters, we have that all closed-loop signals are bounded and the tracking error $e_1 = x_1 - y_d$ exponentially converges to a small region around zero with prescribed performance (4).

Proof. (i) When the controlled system is operating in pattern 0 and controlled by CNEBC u_L^0 for $t_0 \leqslant t < t_{0_j}$, based on (20), (23), and (30), the error systems can be described as

$$\begin{cases} \dot{\zeta}_1 = \varrho\left(-c_1\zeta_1 + \zeta_2 - \tilde{e}_2 + y_2\right), \\ \dot{\zeta}_i = -c_i\zeta_i + \zeta_{i+1} - \zeta_{i-1} + y_{i+1},\ 2 \leqslant i \leqslant n-1, \\ \dot{\zeta}_n = G_\chi^0(-c_n\zeta_n + \bar{W}_U^{0^{\mathrm{T}}} S(Z) - u^{*0}(\bar{x}_n, \nu)) - r\phi^{(n+1)} - \zeta_{n-1}. \end{cases} \tag{46}$$

Consider the Lyapunov function candidate as

$$V^0 = \frac{\zeta_1^2}{2\varrho} + \sum_{i=2}^{n} \frac{1}{2}\zeta_i^2 + \sum_{i=1}^{n-1} \frac{1}{2} y_{i+1}^2. \tag{47}$$

It is easy to see that V^0 is positive definite. We have

$$\begin{aligned} \dot{V}^0 &= \zeta_1\dot{\zeta}_1/\varrho - \frac{\dot{\varrho}}{2\varrho^2}\zeta_1^2 + \sum_{i=2}^{n} \zeta_i\dot{\zeta}_i + \sum_{i=1}^{n-1} y_{i+1}\dot{y}_{i+1} \\ &= -\sum_{i=1}^{n-1} c_i\zeta_i^2 - \frac{\dot{\varrho}}{2\varrho^2}\zeta_1^2 + \sum_{i=1}^{n-1} \zeta_i y_{i+1} - \zeta_1\tilde{e}_2 + \sum_{i=1}^{n-1}\left[-\frac{y_{i+1}^2}{\tau_{i+1}} + y_{i+1}\Phi_{i+1}\right] - G_\chi^k c_n\zeta_n^2 \\ &\quad + G_\chi^k\zeta_n[\bar{W}_U^{0^{\mathrm{T}}} S(Z) - u^{*0}(\bar{x}_n, \nu)] - r\phi^{(n+1)}\zeta_n. \end{aligned} \tag{48}$$

Similar to (A3) in Appendix A, by combining (32) and Young's inequality, the following inequality holds:

$$G_\chi^0\zeta_n[\bar{W}_U^{0^{\mathrm{T}}} S(Z) - u^{*0}(\bar{x}_n, \nu)] \leqslant G_{\max}^{0^2} c_{n1}\zeta_n^2 + \frac{\epsilon^{*0^2}}{4c_{n1}}. \tag{49}$$

Then, combining (A3) and (A4), we can obtain

$$\dot{V}^0 \leqslant -\sum_{i=1}^{n} \Xi'\zeta_i^2 + \sum_{i=1}^{n-1}\left[-\frac{1}{\tau_{i+1}} + \frac{1}{4} + \frac{M_{i+1}^2}{4\omega}\right] y_{i+1}^2 + \beth^0, \tag{50}$$

where $\beth^0 = \epsilon^{*0^2}/4c_{n1} + r^2/4(H_2^2/c_{11} + H_{n+1}^2/c_{n2}) + (n-1)\omega$, $c_1 = \Xi' + c_{11} + 1 - \dot{\varrho}/2\varrho$, $c_i = \Xi' + 1$ $(i = 2, 3, \ldots, n-1)$, $G_{\min}^0 c_n = \Xi' + G_{\max}^{0^2} c_{n1} + c_{n2}$ with Ξ' being a positive design constant, and the time constant is set as $1/\tau_{i+1} = \Xi' + 1/4 + M_{i+1}^2/4\omega$. Similar to Theorem 1, let $\gamma^0 = \min\{2\varrho\Xi', 2\Xi'\}$ and we have

$$\dot{V}^0 \leqslant -\sum_{i=1}^{n} \Xi'\zeta_i^2 - \sum_{i=1}^{n-1} \Xi' y_{i+1}^2 + \beth^0 \leqslant -\gamma^0 V^0 + \beth^0. \tag{51}$$

Then, the following inequality holds:

$$V^0 \leqslant \frac{\beth^0}{\gamma^0} + \left(V^0(0) - \frac{\beth^0}{\gamma^0}\right)\exp(-\gamma^0 t). \tag{52}$$

Similar to the analysis in Theorem 1, it can be concluded that all closed-loop signals are bounded, and the tracking error $e_1 = x_1 - x_{d,1}$ converges exponentially to a small region around zero with PP (4).

(ii) When the control situation changes from the 0th to the jth at time t_{0_j}, and the system dynamics $F^0(\bar{x}_n, u_L^0)$ changes to $F^j(\bar{x}_n, u_L^0)$ $(j \in \{1, 2, \ldots, N\})$ accordingly as given by (44), based on Assumption 2, all the states of the controlled system are uniformly bounded before the change in control situation is

detected. According to the rapid recognition scheme, the sudden change is recognized rapidly at time $t_{0_{j'}}$, where $t_{0_{j'}} > t_{0_j}$ with $[t_{0_j}, t_{0_{j'}}]$ being a short period of time. Based on rapid recognition, the correct candidate experienced controller u^j is quickly selected to control the current controlled system. Considering the moment at which u^j is selected, the NN input value of $\bar{W}_U^{j^{\mathrm{T}}} S(Z)$ embedded in u^j might be beyond the region Ω_{φ_d} as given by (32), i.e., $|\bar{W}_U^{j^{\mathrm{T}}} S(Z) - u^{*j}(\bar{x}_n, \nu)|$ might be a large value; thus, an appropriate high gain experienced controller $u^{j'}$, as given by (45), is implemented first at time $t_{0_{j'}}$, and the system dynamics $F^j(\bar{x}_n, u_L^0)$ changes to $F^j(\bar{x}_n, u_L^{j'})$ accordingly as given by (44). Then, the error systems can be described as

$$\begin{cases} \dot{\zeta}_1 = \varrho\left(-c_1\zeta_1 + \zeta_2 - \tilde{e}_2 + y_2\right), \\ \dot{\zeta}_i = -c_i\zeta_i + \zeta_{i+1} - \zeta_{i-1} + y_{i+1},\ 2 \leqslant i \leqslant n-1, \\ \dot{\zeta}_n = G_\chi^j(-c_n^h\zeta_n + \bar{W}_U^{j^{\mathrm{T}}} S(Z) - u^{*j}(\bar{x}_n, \nu)) - r\phi^{(n+1)} - \zeta_{n-1}, \end{cases} \tag{53}$$

where $c_n^h \gg c_n$ is the high control gain. Consider the Lyapunov function candidate as $V^j = \frac{\zeta_1^2}{2\varrho} + \sum_{i=2}^{n} \frac{1}{2}\zeta_i^2 + \sum_{i=1}^{n-1} \frac{1}{2} y_{i+1}^2$. Similar to the analysis in step (i) of this proof, the large c_n^h is selected to compensate the possible large $|\bar{W}_U^{j^{\mathrm{T}}} S(Z) - u^{*j}(\bar{x}_n, \nu)|$. Then $\beth^j$ as given in (51) can be made very small, and we can obtain

$$V^j \leqslant \frac{\beth^j}{\gamma^j} + \left(V^j(0) - \frac{\beth^j}{\gamma^j}\right) \exp(-\gamma^j t). \tag{54}$$

From (54), we can conclude that the tracking error $e_1 = x_1 - x_{d,1}$ will converge exponentially to a small region around zero with PP (4) quickly; thus, the NN input Z embedded in u_L^j is pulled back to region Ω_{φ_d}. Hereafter, the normal candidate experienced controller u_L^j is selected at time $t_{0_{j''}}$, and the system dynamics $F^j(\bar{x}_n, u_L^{j'})$ changes to $F^j(\bar{x}_n, u_L^j)$ accordingly.

(iii) After a rapid recognition process, the controlled system re-enters a new normal operating stage. That is, the controlled system is currently operating in pattern j and controlled by the experienced controller u_L^j. Therefore, similar to step (i) of this part, the error systems can be described as

$$\begin{cases} \dot{\zeta}_1 = \varrho\left(-c_1\zeta_1 + \zeta_2 - \tilde{e}_2 + y_2\right), \\ \dot{\zeta}_i = -c_i\zeta_i + \zeta_{i+1} - \zeta_{i-1} + y_{i+1},\ 2 \leqslant i \leqslant n-1, \\ \dot{\zeta}_n = G_\chi^j(-c_n\zeta_n + \bar{W}_U^{j^{\mathrm{T}}} S(Z) - u^{*j}(\bar{x}_n, \nu)) - r\phi^{(n+1)} - \zeta_{n-1}. \end{cases} \tag{55}$$

According to step (i) of this part, we obtain that the tracking error e_1 will converge exponentially to a small region around zero with PP (4).

As can be seen from the above analysis, all the closed-loop signals of the pattern-based control system are bounded, and the tracking error $e_1 = x_1 - x_{d,1}$ converges exponentially to a small region around zero with PP (4) even in the presence of changes in control situation.

Remark 3. The proposed pattern-based control scheme distinguishes itself from existing methods (e.g., [20,22,38]). Compared with existing MMAC methods [20,22], which still belong to the category of adaptive control and lack research on knowledge acquisition, the scheme proposed in this article achieves accurate modeling/learning of different control situations, thereby significantly reducing the number of model sets. When the control situation changes suddenly, the type of the current control situation can be rapidly and accurately recognized, and the correct experience-based controller is selected to obtain superior control performance (while in MMAC, the closest controller is first selected, and then the control performance is gradually improved through online adjustment). For the experience-based controllers as given by (33), compared with the adaptive neural controller (28), the constant RBF NNs $\bar{W}_U^{k^{\mathrm{T}}} S(Z)$ are employed instead of the estimated RBF NNs $\hat{W}_U^{k^{\mathrm{T}}} S(Z)$ $(k = 0, 1, \ldots, N)$. Thus, when the same control task recurs, $\bar{W}_U^{k^{\mathrm{T}}} S(Z)$ can rapidly provide an accurate approximation for the unknown dynamics, and no further online parameter estimation is required in the control process, so the improved control performance with faster response and less computation cost can be achieved. Moreover, compared with the previous work [38], this paper proposes a pattern-based control method with PP based on system transformation,

which greatly reduces the complexity of the control design. To be specific, for the controller design of each control situation, the proposed method uses only one NN unit (while n in [38]). In the pattern recognition process, for one change in the control situation, only $N+1$ dynamic estimators are needed to be constructed ($n\times(N+1)$ are required in [38]). Therefore, this study proposes a more effective control method for high-order systems, especially when n and N are large.

5 Simulation studies

In order to show the feasibility of the proposed pattern-based intelligent control approach, we consider the following nonlinear system with three different control situations (patterns):

$$\begin{cases}\dot{x}_1 = f_1^k(x_1,x_2),\\ \dot{x}_2 = f_2^k(\bar{x}_2,u),\ k=0,1,2,\\ y = x_1,\end{cases}\tag{56}$$

where $y=x_1$ is the output of the system, $f_i^k(\cdot)$ $(i=1,2,k=0,1,2)$ denote the unknown nonlinearities corresponding to three different patterns, $f_1^0(x_1,x_2)=x_1+x_2+0.1x_2^3$, $f_2^0(\bar{x}_2,u)=x_1x_2+0.2(1+x_1^2)u+0.1\sin(u)$, $f_1^1(x_1,x_2)=x_1+x_2+0.2(1+x_1^2)x_2^3$, $f_2^1(\bar{x}_2,u)=x_1x_2+0.2(1+x_1^2)u+0.1\sin(u)$, $f_1^2(x_1,x_2)=x_1+x_2+0.4x_2^3$, $f_2^2(\bar{x}_2,u)=x_1x_2+0.15(1+x_2^2)u$. It is easy to prove that system (56) satisfies Assumption 1. Our control objective is to drive the system output y to accurately track the desired reference trajectory $y_d=\sin(t)+\cos(0.5t)$ with guaranteed predefined performance when the plant operating in multiple different control situations. The initial condition is chosen as $[x_1(0),x_2(0)]^{\mathrm{T}}=[1,0]^{\mathrm{T}}$. In this simulation, from (4), we have $-\underline{\varpi}\rho(t)<e_1(t)<\overline{\varpi}\rho(t)$, where $\underline{\varpi}=\overline{\varpi}=1$, the performance function is given as $\rho(t)=(1-0.05)\mathrm{e}^{-1.2t}+0.05$. The observer is defined as

$$\begin{cases}r\dot{\varsigma}_1 = \varsigma_2,\\ r\dot{\varsigma}_2 = -h_1\varsigma_2-\varsigma_1+y(t),\end{cases}\tag{57}$$

where $h_1=2, r=0.01$. According to transformation (11), the transformed system states $\hbar_1=x_1$ and $\hbar_2=\dot{x}_1=f_1^k(x_1,x_2)$ $(k=0,1,2)$. Then, from (57), the state estimate is $\hat{\hbar}=[\varsigma_1,\varsigma_2/r]^{\mathrm{T}}$.

5.1 Simulation of identification

In the first identification phase, the adaptive controller $u^k=-c_2\zeta_2+\hat{W}_U^{k^{\mathrm{T}}}S(Z)$ (as given by (28)) and the corresponding virtual control law $\alpha_2=-c_1\zeta_1+\dot{\rho}(t)/\rho(t)e_1+\dot{y}_d$ are used to achieve learning in the stable adaptive control process, where ζ_1 is defined in (9), $\zeta_2=\varsigma_2/r-\alpha_{2f}$, the first-order filter is designed as $\tau_2\dot{\alpha}_{2f}+\alpha_{2f}=\alpha_2$ with $\tau_2=0.01$. The weight update law is given by (29), and the NN input $Z=[\bar{x}_2^{\mathrm{T}},\nu]^{\mathrm{T}}$, where $\upsilon=-\dot{\alpha}_{2f}+\zeta_1$. In the simulation studies, we construct the Gaussian RBF NN $W_U^{k^{\mathrm{T}}}S(Z)$ using 1053 nodes, with the centers ξ_i evenly spaced on $[-3,3]\times[-3,3]\times[-4.5,4.5]$, the widthes are designed as $\eta_1^k=\eta_2^k=\eta_3^k=0.75$, the design parameters are chosen as $c_1=4$, $c_2=8$, $\Gamma_U^k=8$ and $\sigma_U^k=0.0001$, and the initial weights are set as $\hat{W}_U^k(0)=0, k=0,1,2$.

Simulation results for the first identification phase are given in Figures 3–8. Due to space limitations, only the simulation results of pattern 0 (i.e., $k=0$) are shown here. The simulation results of the other two patterns are similar to these. From Figures 3 and 4, it is seen that the system output tracks the reference trajectory well. Figure 4 shows the output tracking error with and without PP, respectively. The convergence of partial neural weights $\hat{W}_U^0$ is demonstrated in Figure 5. Based on (31), excellent convergence of the neural weights can be obtained when $t=[280,300]$ s, and we have $\bar{W}_U^0=\mathrm{mean}_{t\in[t_{280}^0,t_{300}^0]}\hat{W}_U^0(t)$. Through DL, the implicit desired control dynamics $u^{*0}(Z)$ of the plant can be accurately identified by the learned constant RBF NN $\bar{W}_U^{0^{\mathrm{T}}}S(Z)$, as shown in Figure 6. Using the learned knowledge, a set of pattern-based candidate controllers as given by (33) is constructed. Under the experience-based controller, it is seen from Figure 7 that improved tracking performance can be achieved and the PP is still satisfied.

In the second identification phase, we assume that the plant is initially operating in pattern 0 (which is regarded as the current normal control situation) and is controlled by u^0 (as given by (33), $k=0$).

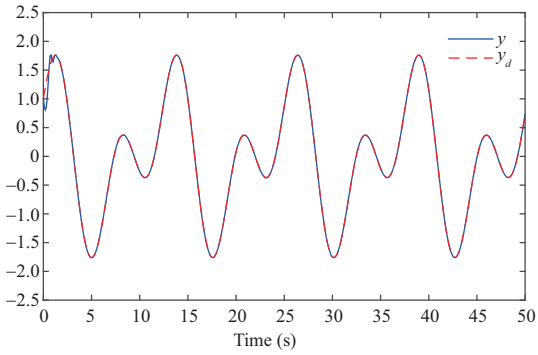

Figure 3 (Color online) System output y and reference signal y_d.

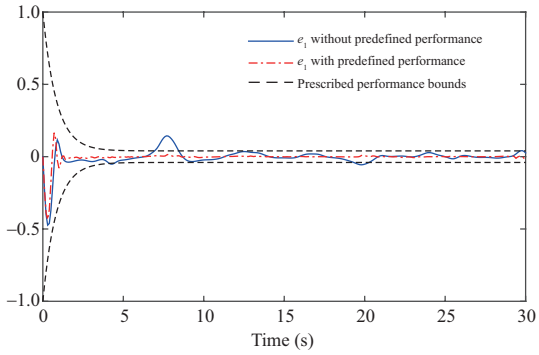

Figure 4 (Color online) Tracking error e_1 of ANC and PP bounds.

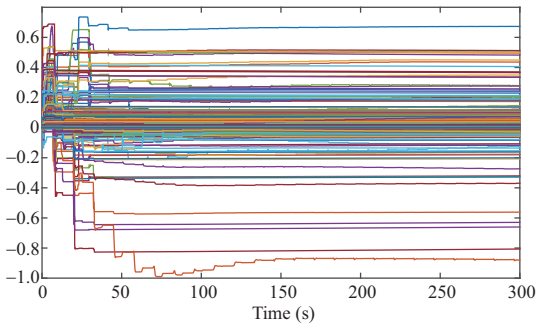

Figure 5 (Color online) Convergence of partial neural weights $\hat{W}_U^0$.

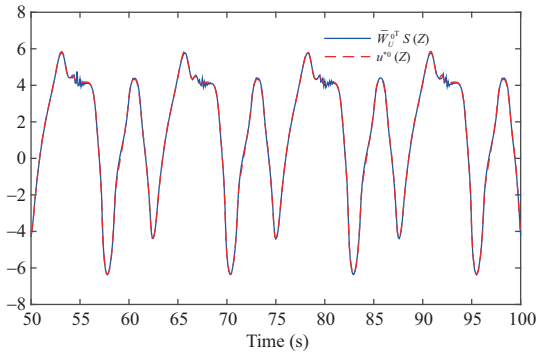

Figure 6 (Color online) Function approximation dynamics trajectory.

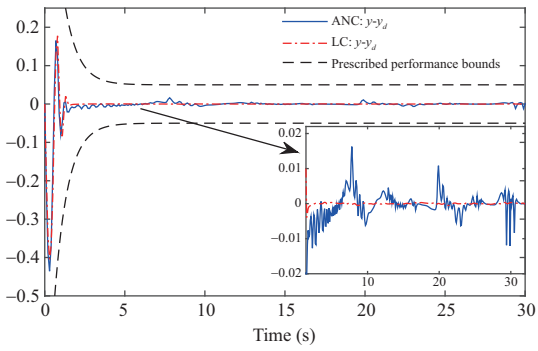

Figure 7 (Color online) Tracking error e_1 of the adaptive neural control and learning control.

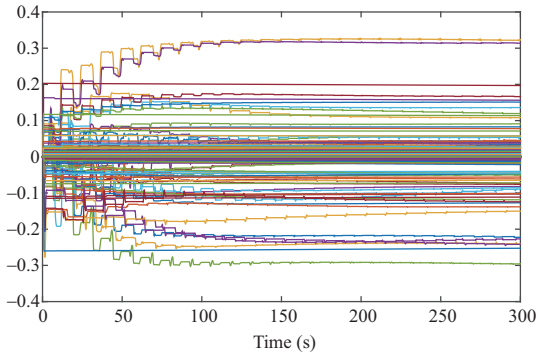

Figure 8 (Color online) Partial parameter convergence $\hat{W}_F^{0,1}$.

Based on the design in Subsection 3.2, in this simulation, we construct the Gaussian RBF network $W_F^{s,k^{\mathrm{T}}} S_F(Z_F)$ using 1053 nodes, with the centers ξ_i evenly spaced on $[-3,3]\times[-3,3]\times[-4.5,4.5]$, and the width is 0.75. The design parameters are set as $a^k=4$, $\Gamma_F^k=5$, $\sigma_F^k=0.0001$. The initial weights $\hat{W}_F^{s,k}=0, s=0,1,2, k=0,1,2$, and the initial states $[x_1(0),x_2(0)]^{\mathrm{T}}=[1,0]^{\mathrm{T}}$.

The simulation results of the second identification phase for pattern 1 under u_L^0 are given in Figures 8 and 9. Figure 8 illustrates the convergence of partial neural weights $\hat{W}_F^{0,1}$, we can see that excellent convergence can be achieved in the last 20 s, and it is obtained that $\bar{W}_F^{0,1}=\mathrm{mean}_{t\in[t'_{280},t'_{300}]}\hat{W}_F^{0,1}(t)$. Through DL, the unknown nonlinear dynamics $F^{0,1}(\bar{x}_2,u_L^0)$ (as defined in (34)) is accurately identified by the learned constant NN $\bar{W}_F^{0,1^{\mathrm{T}}} S_F(\bar{x}_2,u_L^0)$, as shown in Figure 9. In the same way, all the unknown nonlinear dynamics $F^{s,k}(\bar{x}_2,u_L^s), k=0,1,2, s=0,1,2$ are accurately identified by constant

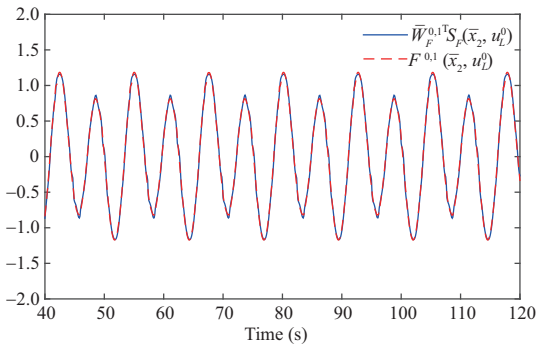

Figure 9 (Color online) System identification: $F^{0,1}(\bar{x}_2, u_L^0)$ and $\bar{W}_F^{0,1^{\mathrm{T}}} S_F(\bar{x}_2, u_L^0)$.

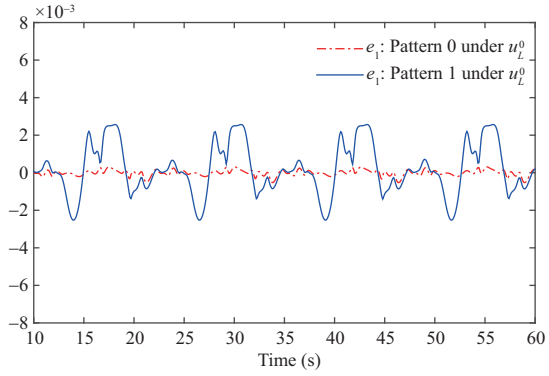

Figure 10 (Color online) Tracking errors of patterns 0 and 1 under u_L^0.

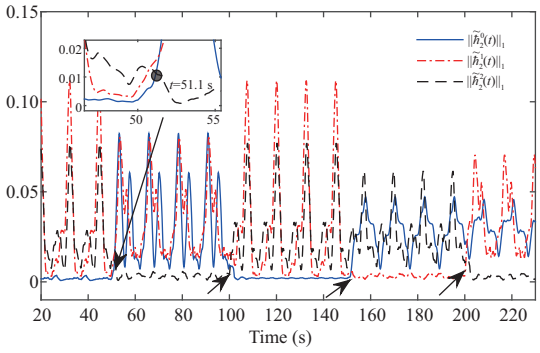

Figure 11 (Color online) Recognition residuals: average L_1 norm $\|\tilde{h}_2^k(t)\|_1$, $k = 0, 1, 2$.

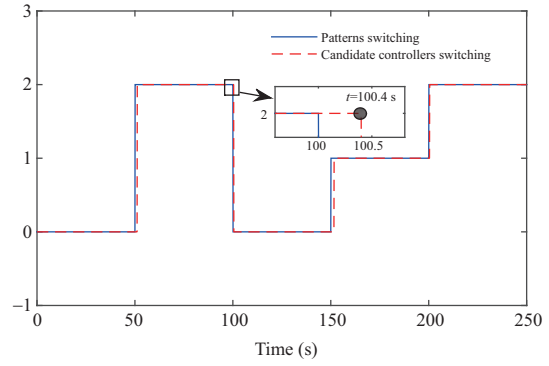

Figure 12 (Color online) Switching sequences of patterns and candidate controllers.

NNs $\bar{W}_F^{s,k^{\mathrm{T}}} S_F(\bar{x}_2, u_L^s)$. By the way, the tracking performance will be poor while the operating plant is controlled by the non-matching controller, for example, the plant operating in pattern 1 but is controlled by u_L^0, as illustrated in Figure 10. Using the learned constant NNs $\bar{W}_F^{s,k^{\mathrm{T}}} S_F(Z_F)$, a set of dynamic estimators representing different control situations (as given by (41)) is constructed as $\dot{\bar{h}}_2^k = -b(\bar{h}_2^k - \varsigma_2/r) + \bar{W}_F^{s,k^{\mathrm{T}}} S_F(Z_F), s = 0, 1, 2, k = 0, 1, 2$.

5.2 Simulation of recognition and pattern-based control

In this simulation, the changing sequence of the control situation (pattern) is set as 0 $(0 < t \leqslant 50) \to$ 2 $(50 < t \leqslant 100) \to 0$ $(100 < t \leqslant 150) \to 1$ $(150 < t \leqslant 200) \to 2$ $(200 < t \leqslant 250)$. The plant is originally operating in pattern 0, and due to some reasons, the control situation may change abruptly at an unknown moment. When the jth ($j \in \{0, 1, 2\}$) control situation (which has been trained in the identification phase) recurs, by comparing the constructed dynamic estimators (41) with the monitored system (34), the recognition residual systems as given by (42) are obtained, where $k = 0, 1, 2, j \in \{0, 1, 2\}, s \in \{0, 1, 2\}$, the design parameter $b = 4$.

When the control situation changes, the corresponding average L_1 norms $\|\tilde{h}_2^k(t)\|_1$ $(k = 0, 1, 2)$ change accordingly. Because there is only one dynamical subsystem in the transformed system (34), only one set of residuals is needed for comparison to achieve rapid recognition, as shown in Figure 11. From Figure 11, it is seen that the first change of the control situation is recognized at $t = 51.1$ s, and then the experience-based candidate controller u_L^2 corresponding to the pattern 2 is selected. As analyzed in Subsection 4.2, a high-gain controller $u_L^{2'}$ (as given by (45)) is first implemented for pattern 2 at time 51.1 s for a short period of time, such that the neural inputs embedded in u_L^2 enter into the approximation region $\Omega_{Z_d}^2$ rapidly, and then u_L^2 is selected at time 52 s to achieve superior tracking performance. The design parameters in (45) are set as $c_1 = 3, c_2 = 7$, $c_1^h = c_2^h = 20$. In the same way, other changes are

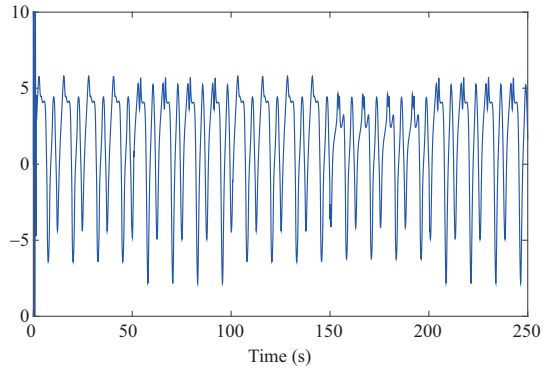

Figure 13 (Color online) Control signal u in the pattern-based control.

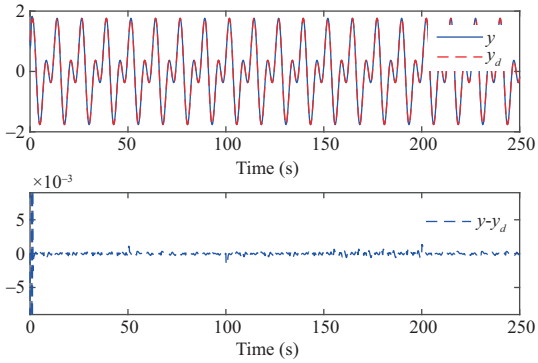

Figure 14 (Color online) Tracking performance with the pattern-based control.

rapidly recognized and the corresponding experience-based candidate controller is correctly selected, as shown in Figures 11 and 12. It is seen from Figure 12 that the correct experience-based controller can be selected rapidly after the change of the control situation. In the entire pattern-based control process, Figure 13 shows the control signal u, and the control performance is illustrated in Figure 14. From the simulation results, it is clear that based on the proposed pattern-based intelligent control scheme, guaranteed stability and improved control performance can be achieved.

Remark 4. It is seen from Theorems 1 and 3 that the tracking and approximation performance is related to the selection of design parameters, including control gain c_i, NN parameters ξ_i, η_i, and l, observer parameters r and h_i, weight update parameters Γ_U, σ_U. The choice of observer parameters needs to satisfy the conditions in Lemma 1, and the choice of other parameters needs to meet the design requirements in theorem analysis. However, the values, such as the upper and lower bounds of $g_i(\cdot)$, ideal neural weight $\|W^*\|$, and ideal approximation error κ^*, are generally unknown, so it is difficult to directly calculate the specific values of the design parameters. For NN parameters, theoretically, in order to achieve good tracking and approximation performance, the center ξ_i, the width η_i, and the node number l of the RBF NN are appropriately chosen so that all neurons cover the entire NN input trajectory. However, how to select these parameters to achieve the optimal tracking and approximation performance is still an open problem. In the simulation studies, the parameters are tuned by a trial-and-error method.

Remark 5. For the proposed pattern-based control scheme, both in the phase of construction of candidate controllers and in the pattern recognition phase, the complexity of the control design has been significantly reduced. From the implementation point of view, for an n-order system, only one NN unit is used to construct the controller, which avoids the recursive analysis process in the PE condition verification process of the neural network. In the pattern recognition phase, only one set of dynamic estimators needs to be constructed to achieve accurate classification for each control situation, which avoids the NN training of each subsystem of the original system (1), and by comparing one set of residuals, sudden changes in control situation can be rapidly recognition, as shown in Figures 11 and 12. As a result, based on the proposed scheme, autonomous learning, decision-making, and high-performance control can be realized in a simpler way. In addition, from the computational point of view, the constructed candidate experience-based controller does not need to adjust any estimated parameters online, and only one NN unit is used for each pattern, which brings numerous benefits in terms of the computational burden. For example, in both ANC and LC of pattern 0, the simulation time is set to 300 s on the same computing device, and the running time is 85 and 29 s, respectively. Using the method in the previous studies (e.g., [30, 38]), the running time is 199 and 105 s, respectively. Therefore, compared with the ANC method in this paper, the LC scheme saves nearly 2/3 of the time, and compared with the existing methods, it saves more than 70% of the time, and the calculation efficiency is significantly improved.

6 Conclusion

This study has proposed a pattern-based intelligent control scheme for pure-feedback systems with PP. In the first identification phase, the original pure-feedback system is simplified into a normal nonaffine

system by a state transformation technique. Based on PP combined with an error transformation method, the proposed HGO-based ANC approach for each control situation not only achieves guaranteed system stability and prescribed tracking control performance using only one NN approximator but also realizes the real learning capability. Accurate identification of the closed-loop dynamics of the transformed system is obtained, an experience-based controller is developed using learned knowledge to achieve improved control performance, and a bank of pattern-based candidate controllers is constructed for different control situations. In the second identification phase, with the HGO, the unknown dynamics of the transformed system is accurately identified, and only one set of dynamic estimators needs to be constructed for the classification of different control situations. In the recognition phase, by comparing the set of dynamic estimators with the monitored system, the change of the control situation at an unknown time can be rapidly recognized based on the minimum residual principle using only one set of residuals. Finally, in the pattern-based control phase, according to the recognition results, the correct candidate experience-based controller is selected to control the plant for superior control performance. The simulation results verified the efficacy of the proposed approach. This study provides a simple general framework for pattern-based control with multiple control situations. Moreover, problems in actual systems, such as input saturation and unknown control directions, which are also important issues, have not been considered. The analysis and design of pattern-based learning and control with input saturation and unknown control directions will be a challenging opportunity for future work.

Acknowledgements This work was supported by Major Program of the National Natural Science Foundation of China (Grant No. 61890922) and Major Basic Program of Shandong Provincial Natural Science Foundation, China (Grant No. ZR2020ZD40).

References

1 Narendra K S, Balakrishnan J. Adaptive control using multiple models. IEEE Trans Automat Contr, 1997, 42: 171–187
2 Fu K S. Learning control systems—review and outlook. IEEE Trans Automat Contr, 1970, 15: 210–221
3 Fu K S, Mendel J M. Adaptive, Learning, and Pattern Recognition Systems: Theory and Applications. Pittsburgh: Academic Press, 1970
4 Lu S W, Basar T. Robust nonlinear system identification using neural-network models. IEEE Trans Neural Netw, 1998, 9: 407–429
5 Wang L Q, Dong J X. Adaptive fuzzy consensus tracking control for uncertain fractional-order multiagent systems with event-triggered input. IEEE Trans Fuzzy Syst, 2022, 30: 310–320
6 Chen W L, Wang J H, Ma K M, et al. Adaptive event-triggered neural control for nonlinear uncertain system with input constraint. Int J Robust Nonlinear Control, 2020, 30: 3801–3815
7 Ge S S, Wang C. Adaptive NN control of uncertain nonlinear pure-feedback systems. Automatica, 2002, 38: 671–682
8 Wang C, Hill D J, Ge S S, et al. An ISS-modular approach for adaptive neural control of pure-feedback systems. Automatica, 2006, 42: 723–731
9 Liu Y J, Zhao W, Liu L, et al. Adaptive neural network control for a class of nonlinear systems with function constraints on states. IEEE Trans Neural Netw Learn Syst, 2021. doi: 10.1109/TNNLS.2021.3107600
10 Xin C, Li Y X, Ahn C K. Adaptive neural asymptotic tracking of uncertain non-strict feedback systems with full-state constraints via command filtered technique. IEEE Trans Neural Netw Learn Syst, 2022. doi: 10.1109/TNNLS.2022.3141091
11 Wu J, Sun W, Su S F, et al. Neural-based adaptive control for nonlinear systems with quantized input and the output constraint. Appl Math Comput, 2022, 413: 126637
12 Lin Z B, Liu Z, Zhang Y, et al. Adaptive neural inverse optimal tracking control for uncertain multi-agent systems. Inf Sci, 2022, 584: 31–49
13 Swaroop D, Hedrick J K, Yip P P, et al. Dynamic surface control for a class of nonlinear systems. IEEE Trans Automat Contr, 2000, 45: 1893–1899
14 Zhang T P, Ge S S. Adaptive dynamic surface control of nonlinear systems with unknown dead zone in pure feedback form. Automatica, 2008, 44: 1895–1903
15 Sui S, Chen C L P, Tong S. Neural-network-based adaptive DSC design for switched fractional-order nonlinear systems. IEEE Trans Neural Netw Learn Syst, 2021, 32: 4703–4712
16 Wang D. Neural network-based adaptive dynamic surface control of uncertain nonlinear pure-feedback systems. Int J Robust Nonlinear Control, 2011, 21: 527–541
17 Bechlioulis C P, Rovithakis G A. Robust adaptive control of feedback linearizable MIMO nonlinear systems with prescribed performance. IEEE Trans Automat Contr, 2008, 53: 2090–2099
18 Bechlioulis C P, Doulgeri Z, Rovithakis G A. Neuro-adaptive force/position control with prescribed performance and guaranteed contact maintenance. IEEE Trans Neural Netw, 2010, 21: 1857–1868
19 Liu Y J, Zeng Q, Tong S, et al. Actuator failure compensation-based adaptive control of active suspension systems with prescribed performance. IEEE Trans Ind Electron, 2020, 67: 7044–7053
20 Ye X D. Nonlinear adaptive control using multiple identification models. Syst Control Lett, 2008, 57: 578–584
21 Han Z, Narendra K S. New concepts in adaptive control using multiple models. IEEE Trans Automat Contr, 2012, 57: 78–89
22 Li X L, Jia C, Liu D X, et al. Nonlinear adaptive control using multiple models and dynamic neural networks. Neurocomputing, 2014, 136: 190–200
23 Antsaklis P J. Intelligent learning control. IEEE Control Syst Mag, 1995, 15: 5–7
24 Wang C, Hill D J. Learning from neural control. IEEE Trans Neural Netw, 2006, 17: 130–146
25 Wang C, Hill D J. Deterministic Learning Theory for Identification, Recognition, and Control. Boca Raton: CRC Press, 2009
26 Liu T F, Wang C, Hill D J. Learning from neural control of nonlinear systems in normal form. Syst Control Lett, 2009, 58: 633–638

27 Wang C, Wang M, Liu T F, et al. Learning from ISS-modular adaptive NN control of nonlinear strict-feedback systems. IEEE Trans Neural Netw Learn Syst, 2012, 23: 1539–1550
28 Dai S L, Wang C, Wang M. Dynamic learning from adaptive neural network control of a class of nonaffine nonlinear systems. IEEE Trans Neural Netw Learn Syst, 2014, 25: 111–123
29 Wang M, Wang C. Neural learning control of pure-feedback nonlinear systems. Nonlinear Dyn, 2015, 79: 2589–2608
30 Wang M, Wang C. Learning from adaptive neural dynamic surface control of strict-feedback systems. IEEE Trans Neural Netw Learn Syst, 2015, 26: 1247–1259
31 Abdelatti M, Yuan C Z, Zeng W, et al. Cooperative deterministic learning control for a group of homogeneous nonlinear uncertain robot manipulators. Sci China Inf Sci, 2018, 61: 112201
32 Wang C, Hill D J. Deterministic learning and rapid dynamical pattern recognition. IEEE Trans Neural Netw, 2007, 18: 617–630
33 Wang C, Chen T R. Rapid detection of small oscillation faults via deterministic learning. IEEE Trans Neural Netw, 2011, 22: 1284–1296
34 Chen T R, Wang C, Chen G R, et al. Small fault detection for a class of closed-loop systems via deterministic learning. IEEE Trans Cybern, 2019, 49: 897–906
35 Wu W M, Wang Q, Yuan C Z, et al. Rapid dynamical pattern recognition for sampling sequences. Sci China Inf Sci, 2021, 64: 132201
36 Chen T R, Zhu Z J, Wang C, et al. Rapid sensor fault diagnosis for a class of nonlinear systems via deterministic learning. IEEE Trans Neural Netw Learn Syst, 2022, 33: 7743–7754
37 Yang F F, Wang C. Pattern-based NN control of a class of uncertain nonlinear systems. IEEE Trans Neural Netw Learn Syst, 2018, 29: 1108–1119
38 Zhang F K, Wang C, Yang F F. Pattern-based NN control for uncertain pure-feedback nonlinear systems. J Franklin Inst, 2019, 356: 2530–2558
39 Krstic M, Kanellakopoulos I, Kokotovic P V. Nonlinear and Adaptive Control Design. New York: Wiley, 1995
40 Powell M J D, The Theory of Radial Basis Functions Approximation in 1990. Oxford: Oxford University Press, 1992
41 Kurdila A J, Narcowich F J, Ward J D. Persistency of excitation in identification using radial basis function approximants. SIAM J Control Optim, 1995, 33: 625–642
42 Zhang F K, Wang C. Deterministic learning from neural control for uncertain nonlinear pure-feedback systems by output feedback. Int J Robust Nonlinear Control, 2020, 30: 2701–2718
43 Behtash S. Robust output tracking for non-linear systems. Int J Control, 1990, 51: 1381–1407
44 Apostol T M. Mathematical Analysis. Boston: Addison-Wesley, 1993
45 Farrell J A. Stability and approximator convergence in nonparametric nonlinear adaptive control. IEEE Trans Neural Netw, 1998, 9: 1008–1020
46 Khalil H. Nonlinear Systems. 3rd ed. Upper Saddle River: Prentice-Hall, 2002

Appendix A Proof of Theorem 1

In this proof, the convergence of the tracking error e_1 with PP (4) is achieved for different control situations, and then accurate identification/learning of the transformed implicit desired control dynamics is further obtained in the stable adaptive control process.

(1) Consider the Lyapunov function candidate as

$$V_\zeta^k = \frac{\zeta_1^2}{2\varrho}+\sum_{i=2}^{n}\frac{1}{2}\zeta_i^2+\frac{1}{2}\tilde{W}_U^{k\mathrm{T}}\Gamma_U^{k^{-1}}\tilde{W}_U^k+\sum_{i=1}^{n-1}\frac{1}{2}y_{i+1}^2. \tag{A1}$$

It is easy to see that V_ζ^k is positive definite. By combining (19), (20), (23), (29), and (30), we have

$$\begin{aligned}\dot{V}_\zeta^k &= \zeta_1\dot{\zeta}_1/\varrho-\frac{\dot{\varrho}}{2\varrho^2}\zeta_1^2+\sum_{i=2}^{n}\zeta_i\dot{\zeta}_i+\tilde{W}_U^{k\mathrm{T}}\Gamma_U^{k^{-1}}\dot{\hat{W}}_U^k+\sum_{i=1}^{n-1}y_{i+1}\dot{y}_{i+1}\\ &= -\sum_{i=1}^{n-1}c_i\zeta_i^2-\frac{\dot{\varrho}}{2\varrho^2}\zeta_1^2+\sum_{i=1}^{n-1}\zeta_i y_{i+1}-\zeta_1\tilde{e}_2+\sum_{i=1}^{n-1}\left[-\frac{y_{i+1}^2}{\tau_{i+1}}+y_{i+1}\Phi_{i+1}\right]-G_\chi^k c_n\zeta_n^2\\ &\quad+G_\chi^k\zeta_n\tilde{W}_U^{k\mathrm{T}}S(Z)-G_\chi^k\zeta_n\kappa^k-r\phi^{(n+1)}\zeta_n-\tilde{W}_U^{k\mathrm{T}}S(Z)\zeta_n-\sigma_U^k\tilde{W}_U^{k\mathrm{T}}\hat{W}_U^k.\end{aligned} \tag{A2}$$

According to Lemma 1 in [27], for the bounded $S(Z)$, there is a limited positive constant s^* satisfying $\|S(Z)\|\leqslant s^*$. By combining Assumption 1, Lemma 1, (19), and the Young's inequality, we have

$$\begin{cases}-\zeta_1\tilde{e}_2=-\zeta_1 r\phi^{(2)}\leqslant c_{11}\zeta_1^2+\frac{r^2H_2^2}{4c_{11}},\\ \zeta_i y_{i+1}\leqslant\zeta_i^2+\frac{y_{i+1}^2}{4},\\ G_\chi^k\tilde{W}_U^{k\mathrm{T}}S(Z)\zeta_n\leqslant\frac{s^{*2}G_{\max}^{k2}\zeta_n^2}{\sigma_U^k}+\frac{\sigma_U^k\tilde{W}_U^{k\mathrm{T}}\tilde{W}_U^k}{4},\\ -G_\chi^k\zeta_n\kappa^k\leqslant G_{\max}^{k2}c_{n1}\zeta_n^2+\frac{\kappa^{*k2}}{4c_{n1}},\\ -\tilde{W}_U^{k\mathrm{T}}S(Z)\zeta_n\leqslant\frac{s^{*2}\zeta_n^2}{\sigma_U^k}+\frac{\sigma_U^k\tilde{W}_U^{k\mathrm{T}}\tilde{W}_U^k}{4},\\ -r\phi^{(n+1)}\zeta_n\leqslant c_{n2}\zeta_n^2+\frac{r^2H_{n+1}^2}{4c_{n2}}.\end{cases} \tag{A3}$$

Noticing that $\tilde{W}_U^k=\hat{W}_U^k-W_U^{*k}$ and $\|\Phi_i\|<M_i$, we have $-\sigma_U^k\tilde{W}_U^{k\mathrm{T}}\hat{W}_U^k=-\sigma_U^k\tilde{W}_U^{k\mathrm{T}}W_U^{*k}-\sigma_U^k\tilde{W}_U^{k\mathrm{T}}\tilde{W}_U^k$. Consider the following inequalities:

$$\begin{cases}-\tilde{W}_U^{k\mathrm{T}}\sigma_U^kW_U^{*k}\leqslant\sigma_U^k\|W_U^{*k}\|^2+\frac{\sigma_U^k\tilde{W}_U^{k\mathrm{T}}\tilde{W}_U^k}{4},\\ y_{i+1}\Phi_{i+1}\leqslant\frac{M_{i+1}^2y_{i+1}^2}{4\omega}+\omega.\end{cases} \tag{A4}$$

By substituting (A3) and (A4) into (A2), we have

$$\begin{aligned}\dot{V}_\zeta^k \leqslant & -\sum_{i=1}^{n-1} c_i\zeta_i^2 + \sum_{i=1}^{n-1}\zeta_i^2 + c_{11}\zeta_1^2 - \frac{\dot{\varrho}}{2\varrho^2}\zeta_1^2 + \sum_{i=1}^{n-1}\left[-\frac{1}{\tau_{i+1}} + \frac{1}{4} + \frac{M_{i+1}^2}{4\omega}\right] y_{i+1}^2 \\ & + \left[-G_{\min}^k c_n + (G_{\max}^{k^2}s^{*2} + s^{*2})/\sigma_U^k + G_{\max}^{k^2}c_{n1} + c_{n2}\right]\zeta_n^2 - \frac{\sigma_U^k \tilde{W}_U^{k^{\mathrm{T}}}\tilde{W}_U^k}{4} + \urcorner^k, \end{aligned} \tag{A5}$$

where $\urcorner^k = \sigma_U^k\|W_U^{*k}\|^2 + \kappa^{*k^2}/4c_{n1} + r^2/4(H_2^2/c_{11} + H_{n+1}^2/c_{n2}) + (n-1)\omega$. The corresponding design parameters are chosen as $c_1 = \Xi + c_{11} + 1 - \frac{\dot{\varrho}}{2\varrho}$, $c_i = \Xi + 1$ $(i = 2, 3, \ldots, n-1)$, $G_{\min}^k c_n = \Xi + G_{\max}^{k^2}c_{n1} + c_{n2} + (G_{\max}^{k^2}s^{*2} + s^{*2})/\sigma_U^k$. Let $\Xi = \sigma_U^k/4\lambda_{\max}(\Gamma_U^{-1^k})$ with Ξ being a positive design constant, and the time constant is chosen inductively as $1/\tau_{i+1} = \Xi + 1/4 + M_{i+1}^2/4\omega$. Let $\gamma = \min\{2\varrho\Xi, 2\Xi\}$ and we have

$$\begin{aligned}\dot{V}_\zeta^k &\leqslant -\sum_{i=1}^{n}\Xi\zeta_i^2 - \Xi\tilde{W}_U^{k^{\mathrm{T}}}\lambda_{\max}(\Gamma_U^{-1^k})\tilde{W}_U^k - \sum_{i=1}^{n-1}\Xi y_{i+1}^2 + \urcorner^k \\ &\leqslant -\gamma V_\zeta^k + \urcorner^k. \end{aligned} \tag{A6}$$

Then, the following inequality holds:

$$V_\zeta^k \leqslant \frac{\urcorner^k}{\gamma} + \left(V_\zeta^k(0) - \frac{\urcorner^k}{\gamma}\right)\exp(-\gamma t). \tag{A7}$$

Therefore, by combining (A1) and (A7), ζ_i $(i = 1, 2, \ldots, n)$, y_{j+1} $(j = 1, 2, \ldots, n-1)$, and $\tilde{W}_U^k$ are uniformly bounded. Furthermore, we obtain that $\hat{W}_U^k$ is bounded due to $\hat{W}_U^k = W_U^{*k} + \tilde{W}_U^k$ as well as the boundedness of W_U^k. Since $\zeta_1, x_{d,1}$, and $x_{d,2}$ are bounded and $e_1 = x_1 - x_{d,1}$, x_1 and α_2 are bounded. Owing to the boundedness of y_2 and $y_2 = \alpha_{2f} - \alpha_2$, one has that α_{2f} is bounded. Furthermore, since ζ_2 is bounded and $\zeta_2 = \varsigma_2/r - \alpha_{2f}$, we obtain that ς_2/r is bounded. Based on Lemma 1, ς_2/r converges to $\hbar_2$; thus, it follows that $\hbar_2$ is bounded. According to (11), we have that x_2 is bounded. In the similar way, we can obtain that the states $x_i, \hbar_i, i = 3, 4, \ldots, n$ and the control u^k $(k \in \{0, 1, 2, \ldots, N\})$ corresponding to the kth control situation are all bounded.

Furthermore, by combining (A1) and (A7), we can obtain that, given any $\varepsilon > \sqrt{2\urcorner^k/\gamma}$, there exists a finite time T^k such that, for all $t \geqslant T^k$, the unconstrained error ζ_1 satisfies $|\zeta_1| \leqslant \varepsilon$. That is, ζ_1 can converge to a small region around zero in a finite time T^k since ε can be made arbitrarily small by appropriately choosing the design parameters. By recalling (4) and (6), we can conclude that the system output tracking error e_1 will converge to a small region around zero in a finite time T^k according to PP (4).

(2) Accurate convergence of the estimated parameters commonly requires the satisfaction of PE condition[1)], which is also the basic factor for the occurrence of learning [2]. In this part, accurate convergence of the estimated neural weight $\hat{W}_U^k$ to the ideal weight W_U^{*k} will be obtained. To solve this issue, on the basis of results in [24], a partial PE condition of $S_\zeta(Z)$ is required. Therefore, we need to verify first that all the signals in $Z = [\bar{x}_n^{\mathrm{T}}, \nu]^{\mathrm{T}}$ are recurrent. From step (1) of this proof, $e_1 = x_1 - x_{d,1}$ converges to a small region around zero with PP (4) for $t > T^k$; thus, x_1 will be a recurrent signal with the same period as the recurrent reference signal $x_{d,1}$. According to the exponential convergence of ζ_1, e_1 and y_2, from (17), we can conclude that α_2 follows the recurrent signal $x_{d,2}$. Because $y_2 = \alpha_{2f} - \alpha_2$, α_{2f} also becomes a recurrent signal with the same period as α_2. Due to the exponential convergence of ζ_2 and $\zeta_2 = \varsigma_2/r - \alpha_{2f}$, ς_2/r becomes a recurrent signal with the same period as α_{2f}. Thereafter, based on Lemma 1, $\hbar_2$ becomes a recurrent signal with the same period as ς_2/r. From the system transformation as given by (11), we can conclude that x_2 is also a recurrent signal. Similarly and recursively, the states x_i $(i = 3, 4, \ldots, n)$ and ν are all recurrent signals. From the above analysis, we obtain that the NN input $Z = [\bar{x}_n^{\mathrm{T}}, \nu]^{\mathrm{T}}$ is recurrent, and then the partial PE condition of the regressor subvector $S_\zeta(Z)$ is established.

By employing the localized RBF network along the recurrent trajectory $Z(t)$ $(t > T^k)$, and combining (30) and (29), we have

$$\begin{cases} \dot{\zeta}_n = G_\chi^k(-c_n\zeta_n + \tilde{W}_{U\zeta}^{k^{\mathrm{T}}}S_\zeta(Z) + \kappa_\zeta^k) - r\phi^{(n+1)} - \zeta_{n-1}, \\ \dot{\tilde{W}}_{U\zeta}^k = \dot{\hat{W}}_{U\zeta}^k = -\Gamma_{U\zeta}^k[S_\zeta(Z)\zeta_n + \sigma_U^k\hat{W}_{U\zeta}^k], \end{cases} \tag{A8}$$

and

$$\dot{\tilde{W}}_{U\bar{\zeta}}^k = \dot{\hat{W}}_{U\bar{\zeta}}^k = -\Gamma_{U\bar{\zeta}}^k\left[S_{\bar{\zeta}}(Z)s_n + \sigma_1\hat{W}_{U\bar{\zeta}}^k\right],$$

where $S_\zeta(Z)$ denotes the subvector of $S(Z)$, consisting of Gaussian basis functions close to the trajectory $Z(t)$, and $\hat{W}_{U\zeta}$ denotes the corresponding NN weight subvector. Furthermore, the subscript $(\cdot)_{\bar{\zeta}}$ denotes the region far away from the trajectory $Z(t)$; thus, we obtain that $|\hat{W}_{U\bar{\zeta}}^{k^{\mathrm{T}}}S_{\bar{\zeta}}(Z)|$ is small. $\kappa_\zeta^k = \tilde{W}_{U\bar{\zeta}}^{k^{\mathrm{T}}}S_{\bar{\zeta}}(Z) - \kappa^k$ denotes the neural approximation error along $Z(t)$ with $|\kappa_\zeta^k|$ being close to $|\kappa^{*k}|$. Since ζ_{n-1} exponentially converges to the vicinity around zero, $|r\phi^{(n+1)} + \zeta_{n-1}|$ can be very small by selecting a small enough r. Letting $\bar{\zeta} = \zeta_n/G_{\max}^k$, Eq. (A8) can be rewritten as the following linear time-varying (LTV) system form with a small perturbation:

$$\begin{bmatrix} \dot{\bar{\zeta}} \\ \dot{\tilde{W}}_{U\zeta}^k \end{bmatrix} = \left[\begin{array}{c|c} -c_nG_\chi^k & G_\chi^kS_\zeta^{\mathrm{T}}(Z)/G_{\max}^k \\ \hline -\Gamma_{U\zeta}^kS_\zeta G_{\max}^k & 0 \end{array}\right]\begin{bmatrix} \bar{\zeta} \\ \tilde{W}_{U\zeta}^k \end{bmatrix} + \begin{bmatrix} \kappa_\zeta'^k \\ -\sigma_U^k\Gamma_{U\zeta}^k\hat{W}_{U\zeta}^k \end{bmatrix}, \tag{A9}$$

where $\kappa_\zeta'^k = (G_\chi^k\kappa_\zeta^k - r\phi^{(n+1)} - \zeta_{n-1})/G_{\max}^k$. According to Assumption 1, the convergence of ζ_{n-1}, $\kappa_\zeta'^k$, and $\sigma_U^k\Gamma_{U\zeta}^k\hat{W}_{U\zeta}^k$ can be very small by choosing enough small r and σ_U^k. Noticing that $S_\zeta(Z)$ satisfies the partial PE condition, according to Definition 1 of [27], $G_\chi^kS_\zeta^{\mathrm{T}}(Z)/G_{\max}^k$ also satisfies the PE condition. Define $A^k(t) = -c_nG_\chi^k$ and select $P^k(t) = G_{\max}^{k^2}/G_\chi^k$. Then $\dot{P}^k + P^kA^k + A^{k^{\mathrm{T}}}P^k = -\dot{G}_\chi^kG_{\max}^{k^2}/G_\chi^{k^2} - 2c_nG_{\max}^{k^2}$. From step (1) of this proof, $\bar{x}_n, \hat{W}_U^k$, and u^k are bounded. By combining

1) Narendra K S, Annaswamy A M. Stable Adaptive Systems. Upper Saddle River: Prentice Hall, 1989.

$0 < G^k_{\min} \leqslant G^k_\chi \leqslant G^k_{\max}$ and (25), there is a constant $\bar{G}^k$ satisfying $|\dot{G}^k_\chi| \leqslant \bar{G}^k$. Therefore, we can easily obtain $2c_n + \dot{G}^k_\chi / G^{k^2}_\chi > 0$ by selecting an appropriate c_n. Furthermore, according to Lemma 1 in [26], exponential stability of (A9) is achieved and $\tilde{W}^k_{U\zeta}$ converges to the vicinity around zero with the convergence region being determined by κ'^k_ζ and $\sigma^k_U \Gamma^k_{U\zeta} \hat{W}^k_{U\zeta}$, which both are small values. That is, $\hat{W}^k_{U\zeta}$ could converge accurately to a small region around the ideal $W^{*k}_{U\zeta}$. And then, accurate identification/learning of $u^{*k}(\bar{x}_n, \nu)$ is obtained by $\hat{W}^{k\mathrm{T}}_{U\zeta} S_\zeta(Z)$ and $\bar{W}^{k\mathrm{T}}_U S(Z)$ as

$$u^{*k}(\bar{x}_n, \nu) = \hat{W}^{k\mathrm{T}}_{U\zeta} S_\zeta(Z) + \kappa^k_\zeta = \bar{W}^{k\mathrm{T}}_U S(Z) + \bar{\kappa}^k, \tag{A10}$$

where κ^k_ζ and $\bar{\kappa}^k$ are close to κ^{*k}, and $\bar{W}^{k\mathrm{T}}_U S(Z)$ denotes the constant NN as given by (31).